Gravitational lensing

Volker Perlick
(ZARM, U Bremen, Germany)

from the movie "Interstellar"

II Mesoamerican Workshop on Cosmology and Gravity
Tuxtla Gutierrez, 24–26 October 2018

Outline

1. History of lensing
2. The weak-field formalism of lensing
3. Schwarzschild lensing and generalisations to other spherically symmetric and static spacetimes
4. Kerr lensing and generalisations to other non-static spacetimes

P. Schneider, J. Ehlers, E. Falco:
"Gravitational lenses" Springer (1992)

VP: "Gravitational lensing from a spacetime perspective"
Living Rev. Relativity 7, (2004),
http://www.livingreviews.org/lrr-2004-9

VP: "Gravitational lensing" Lecture Notes,
downloadable from VP's homepage

1. History of lensing

Newtonian light deflection:

Henry Cavendish 1786, Johann v. Soldner 1801

Henry Cavendish
(1731 – 1810)

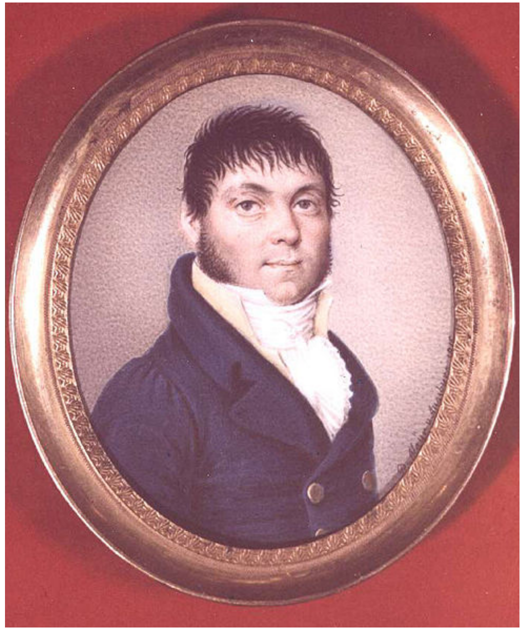

Johann v. Soldner
(1776 –1833)

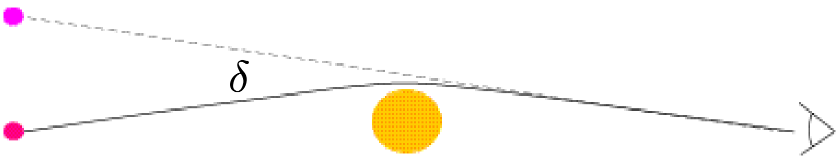

$$\delta = \frac{2\,G\,M}{c^2\,R}, \quad \delta_\odot = 0.87''$$

Einsteinian light deflection:
Albert Einstein 1915

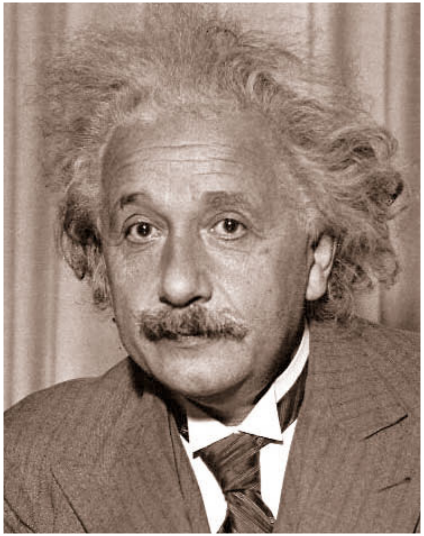

Albert Einstein
(1879-1955)

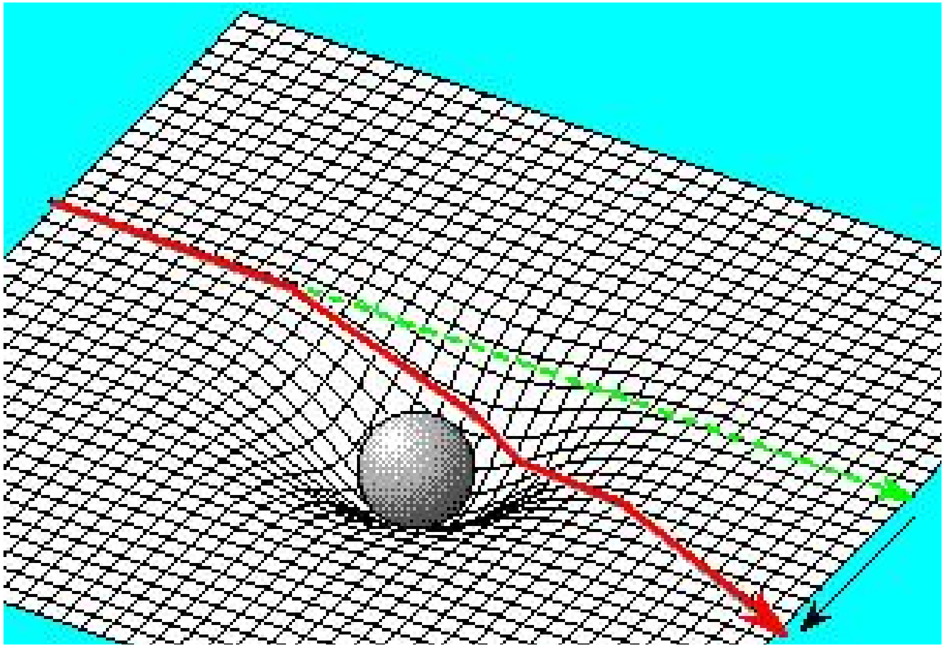

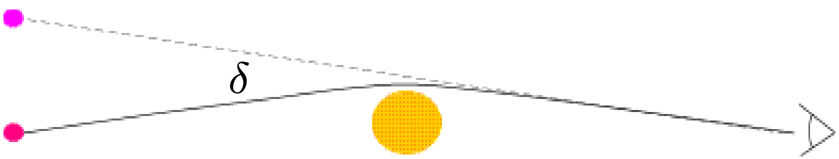

$$\delta = \frac{4\,G\,M}{c^2\,R}, \quad \delta_\odot = 1.73''$$

Confirmation of Einsteinian light deflection:
Arthur S. Eddington 1919

Arthur S. Eddington
(1882 – 1944)

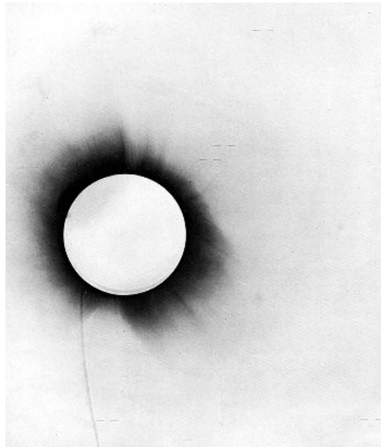

Solar eclipse 1919

Principe: $\delta = 1.61'' \pm 0.40''$, **Sobral:** $\delta = 1.98'' \pm 0,16''$

D. Lebach et al. (1995): $\left|\frac{\delta - \delta_{\text{Einstein}}}{\delta_{\text{Einstein}}}\right| \leq 0.02\,\%$

Simulation with plastic lens:

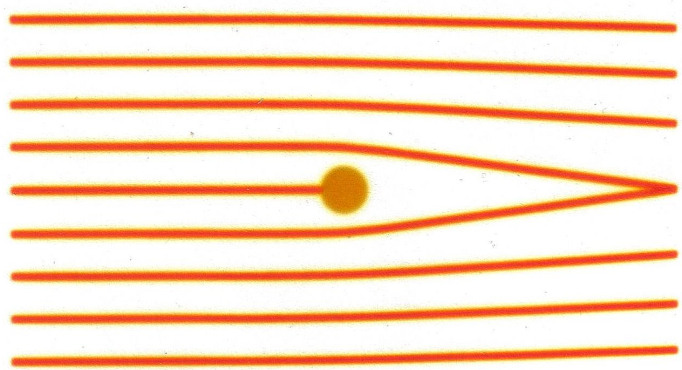

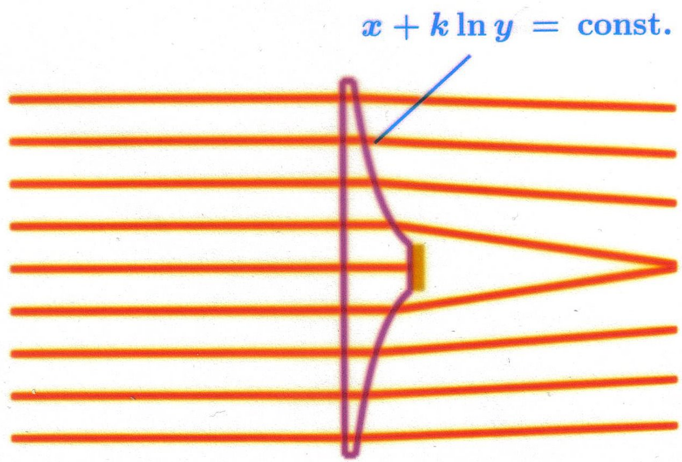

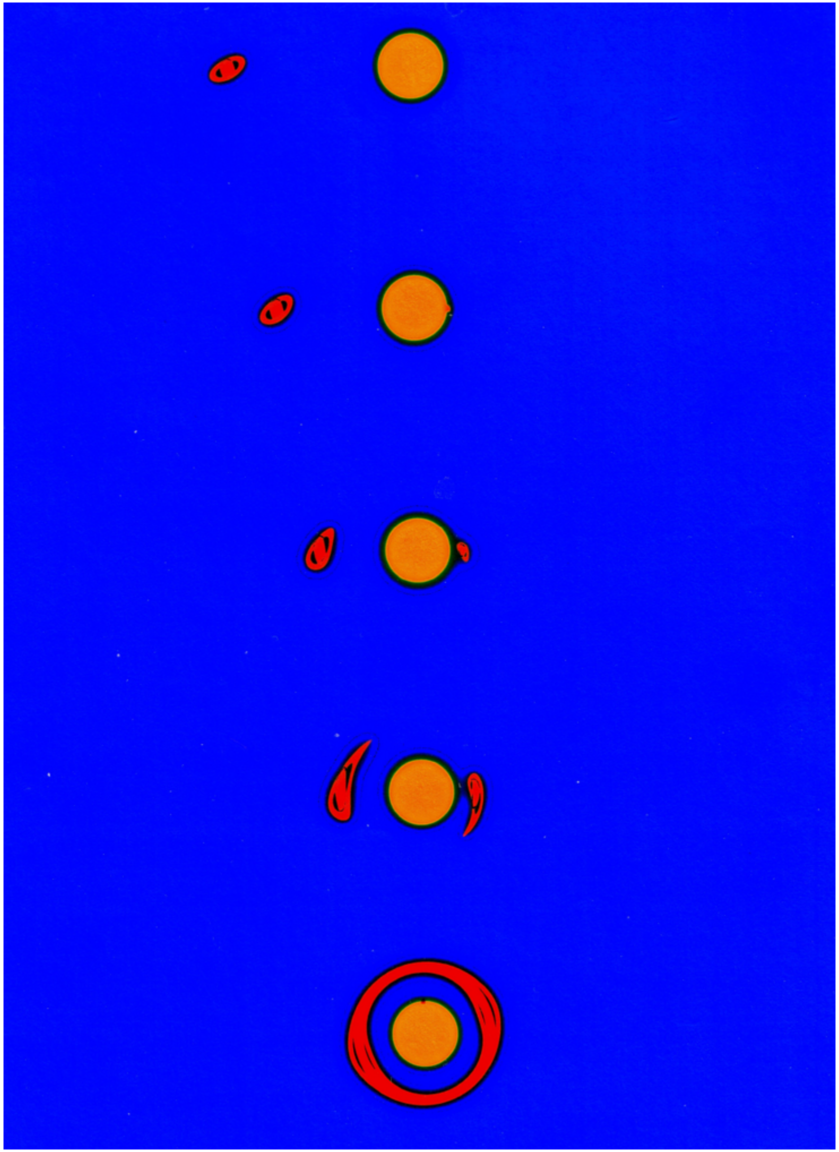

Are multiple images or rings observable?

star lensed by star	Albert Einstein (1936): practically impossible to observe
galaxy lensed by galaxy	Fritz Zwicky (1937): very well possible to observe

Fritz Zwicky
(1898 – 1974)

Observation of multiple imaging:

D. Walsh, R. Carlswell, R. Weyman (1979)

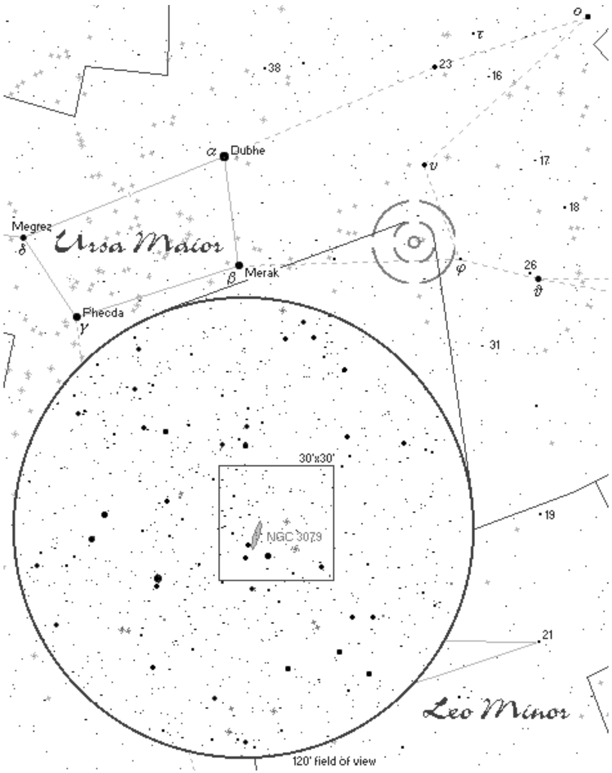

Double quasar QS0 0957 +561

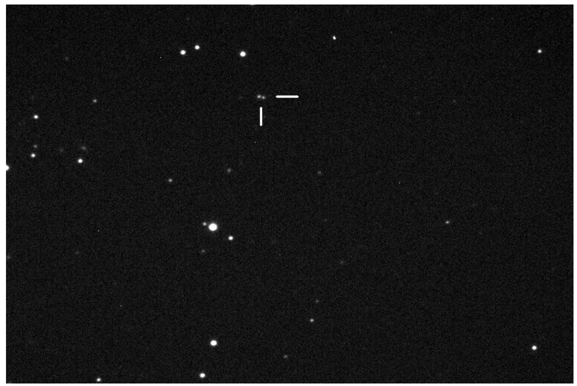

angular separation $= \ 6''$

magnitude $= \ 17^{\mathrm{m}}$

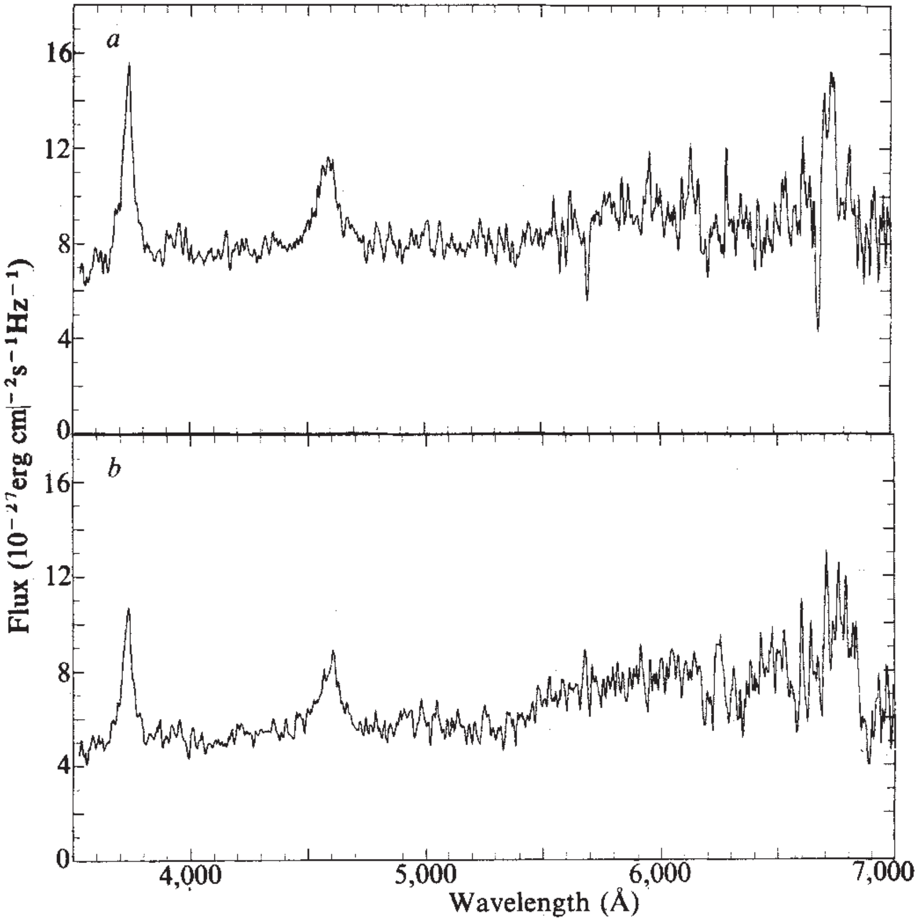
a
b
Flux (10^{-27}erg cm^{-2}s^{-1}Hz^{-1})
0
4
8
12
16
4,000
5,000
6,000
7,000
Wavelength (Å)

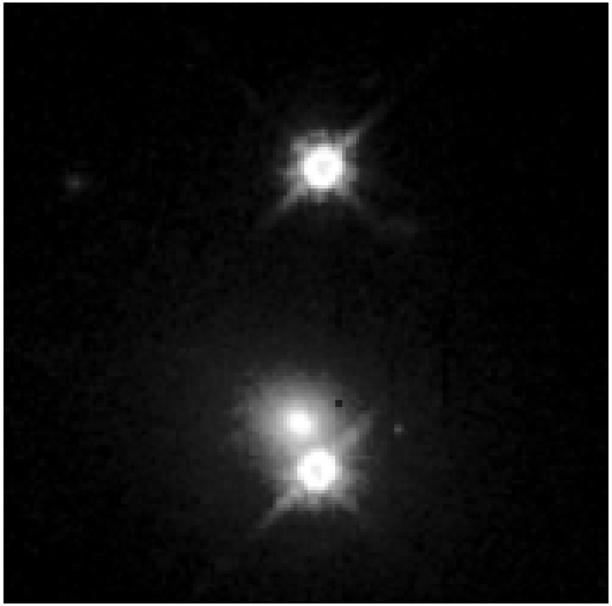

Redshift of quasar images: $z_Q = 1.4$

Redshift of galaxy (lens): $z_L = 0.4$

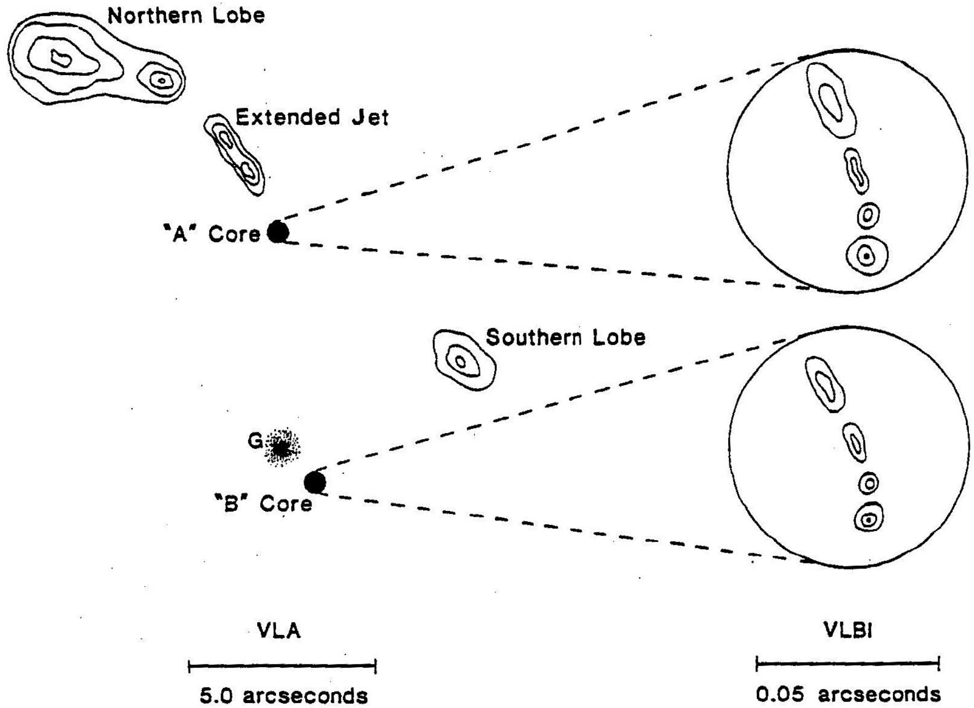
Northern Lobe
Extended Jet
"A" Core
Southern Lobe
G
"B" Core
VLA
5.0 arcseconds
VLBI
0.05 arcseconds

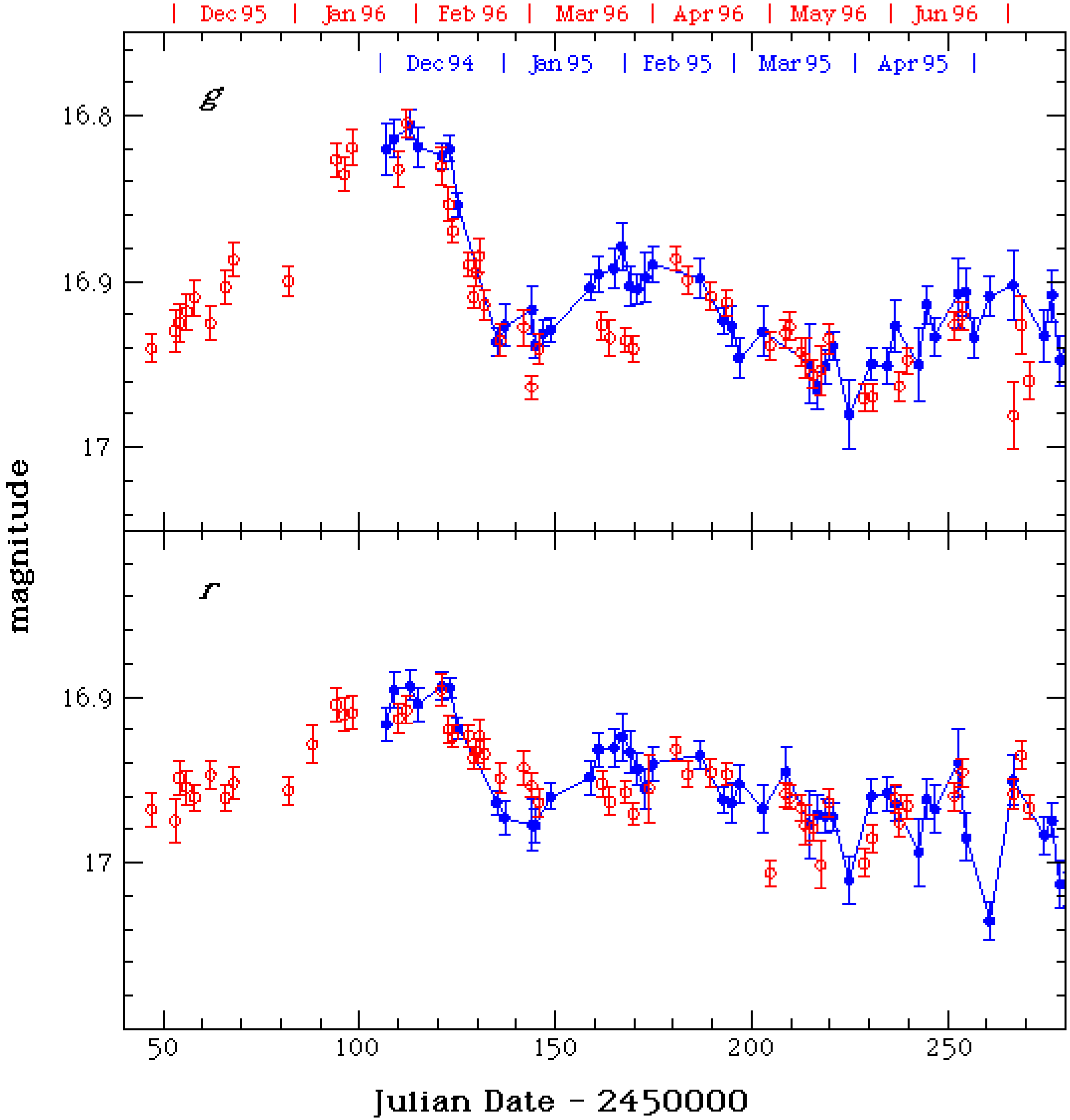
Dec 95
Jan 96
Feb 96
Mar 96
Apr 96
May 96
Jun 96
Dec 94
Jan 95
Feb 95
Mar 95
Apr 95
g
r
16.8
16.9
17
magnitude
50
100
150
200
250
Julian Date - 2450000

Q 2237 +030 (“Einstein Cross ”)

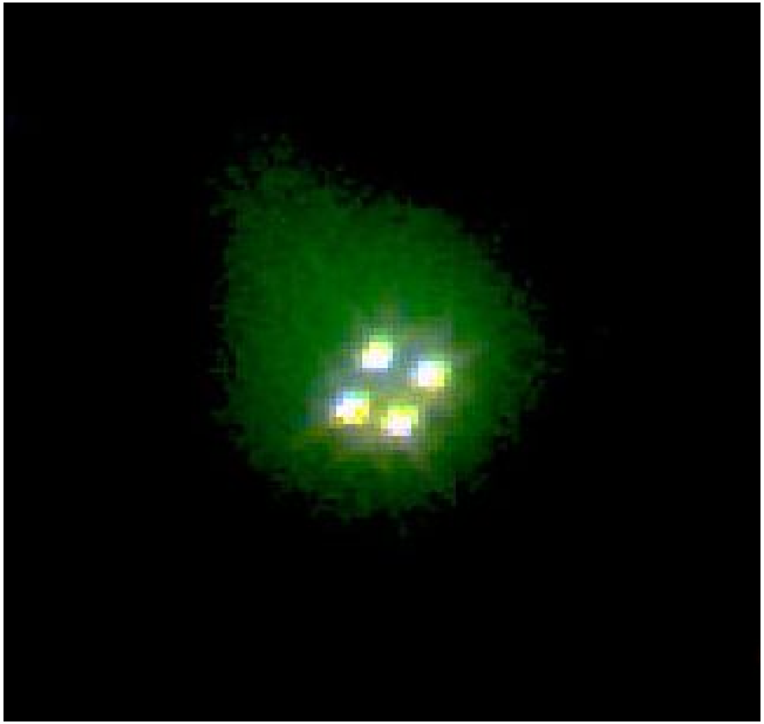

H 1413+1143 ("Clover Leaf")

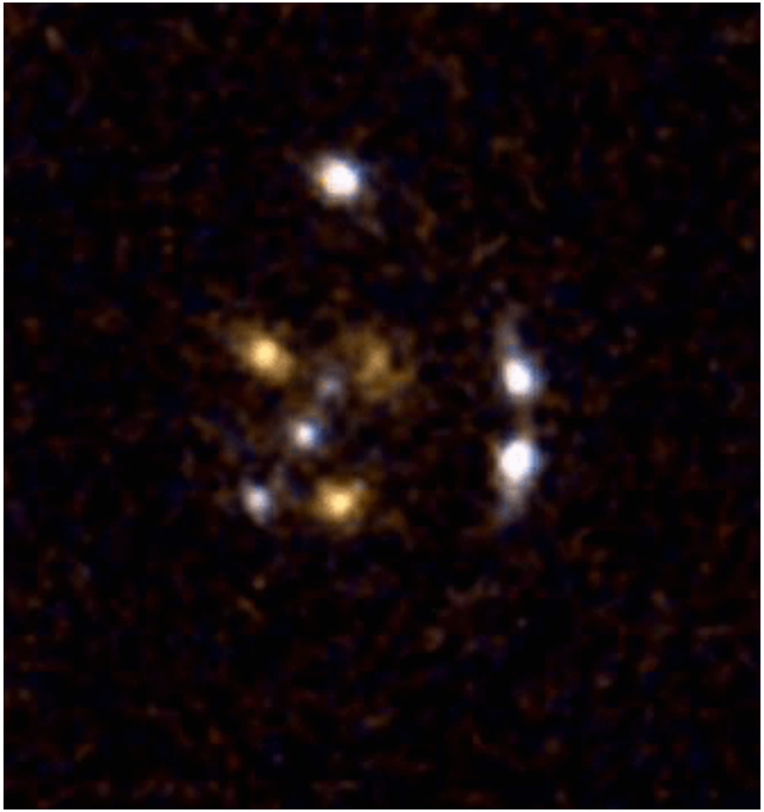

B 1359 +154 (six images, three deflectors)

Observation of Einstein rings:

J. Hewitt et al. (1988)

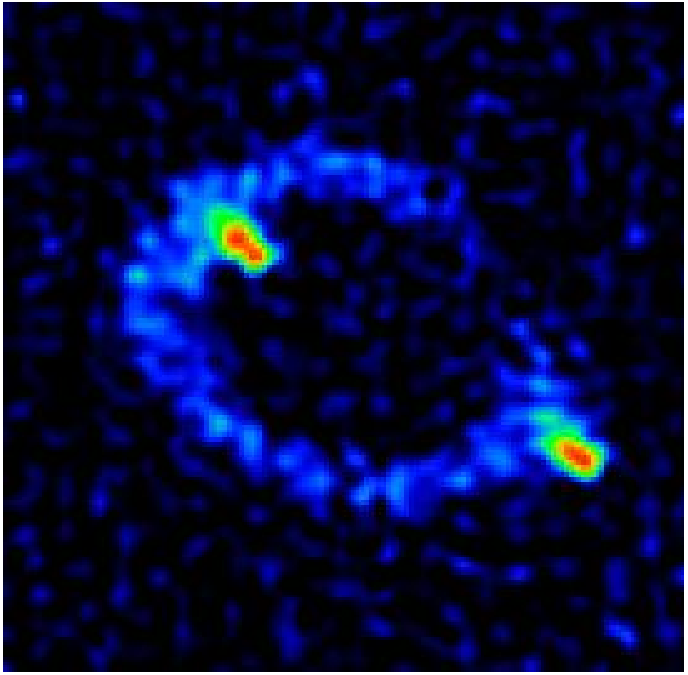

MG 1131 +0456

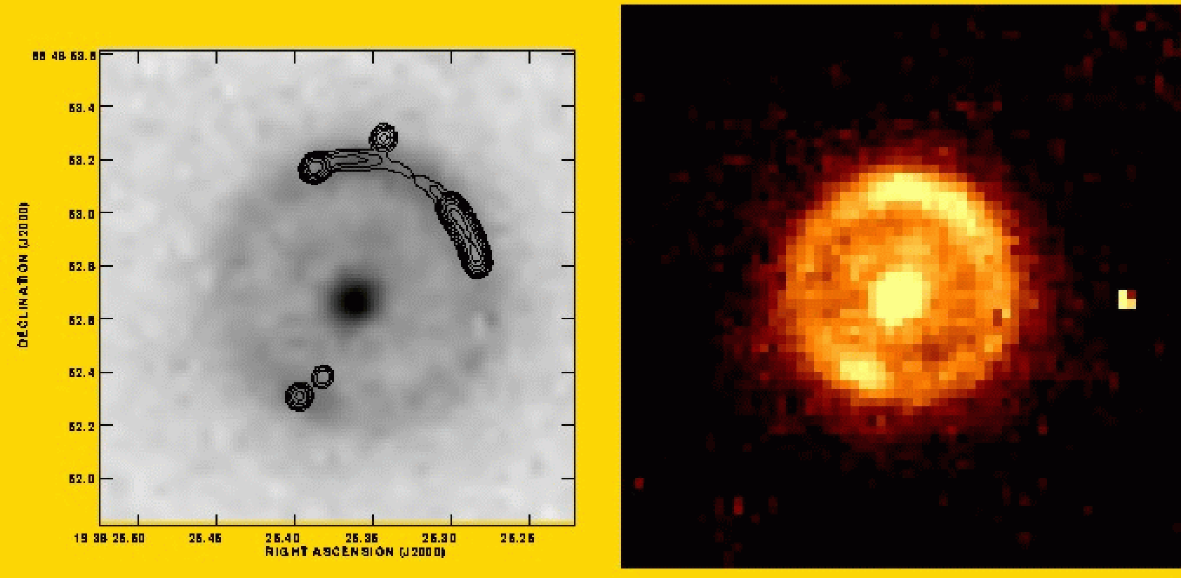

The gravitational lens JVAS B1938+666

Left: HST/NICMOS greyscale with MERLIN radio contours

Right: Colour image of the HST/NICMOS image

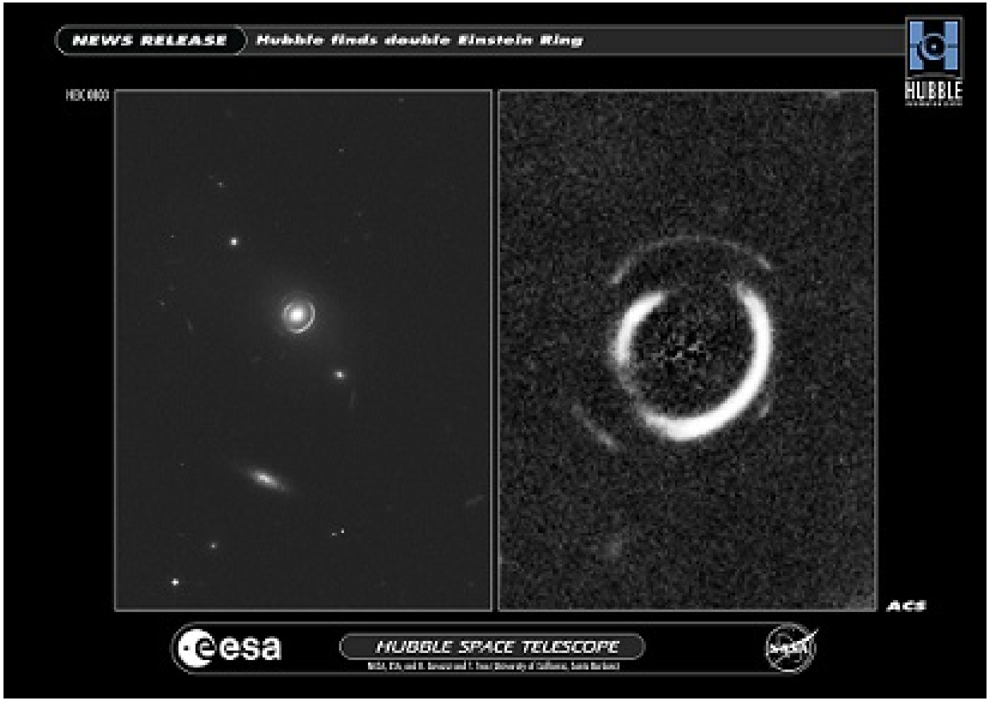

SDSS J0946+1006

Observation of giant luminous arcs:

R. Lynds, V. Petrosian (1986), G. Soucail et al. (1987)

Abell 370

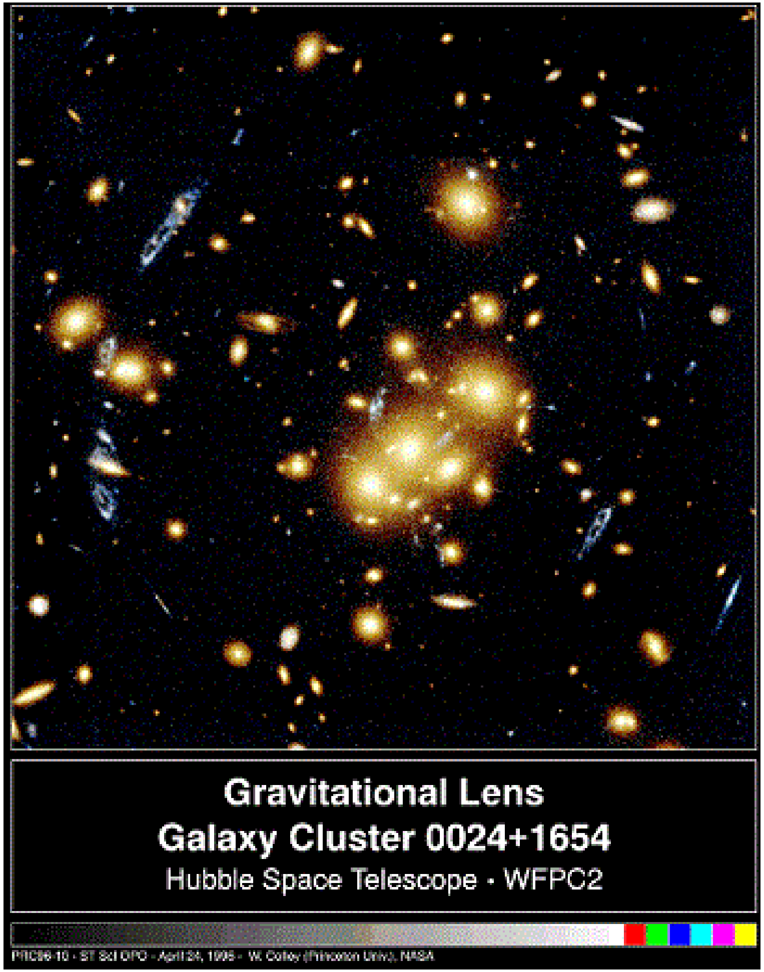
Gravitational Lens
Galaxy Cluster 0024+1654
Hubble Space Telescope · WFPC2

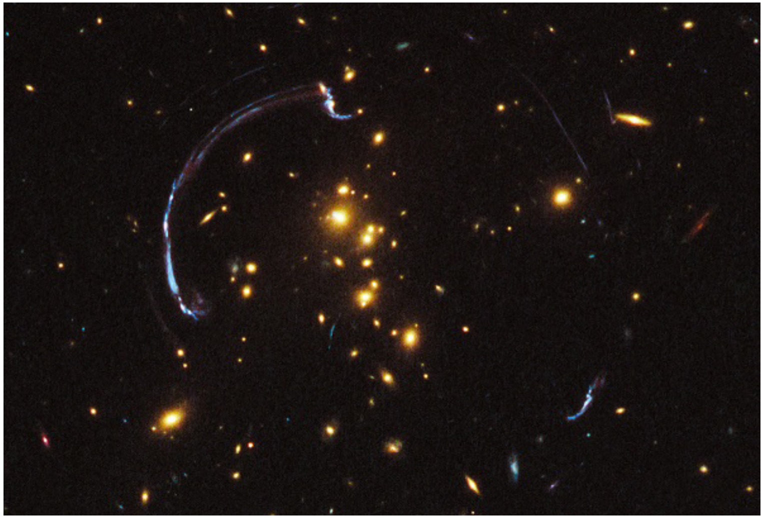

RCS2 032727-132623

Weak lensing:
A tool for detecting dark matter in galaxy clusters
A. Tyson et al. (1990)

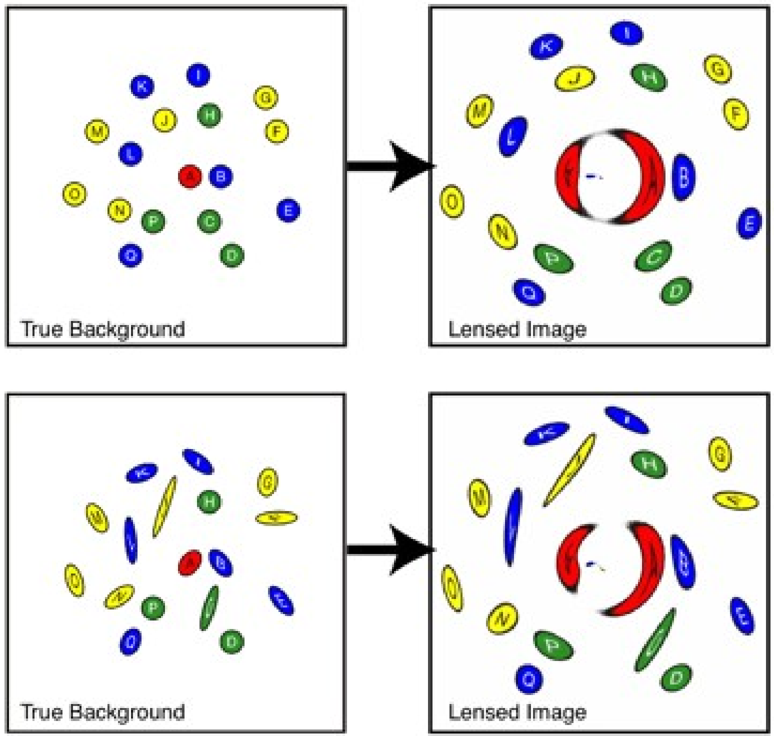

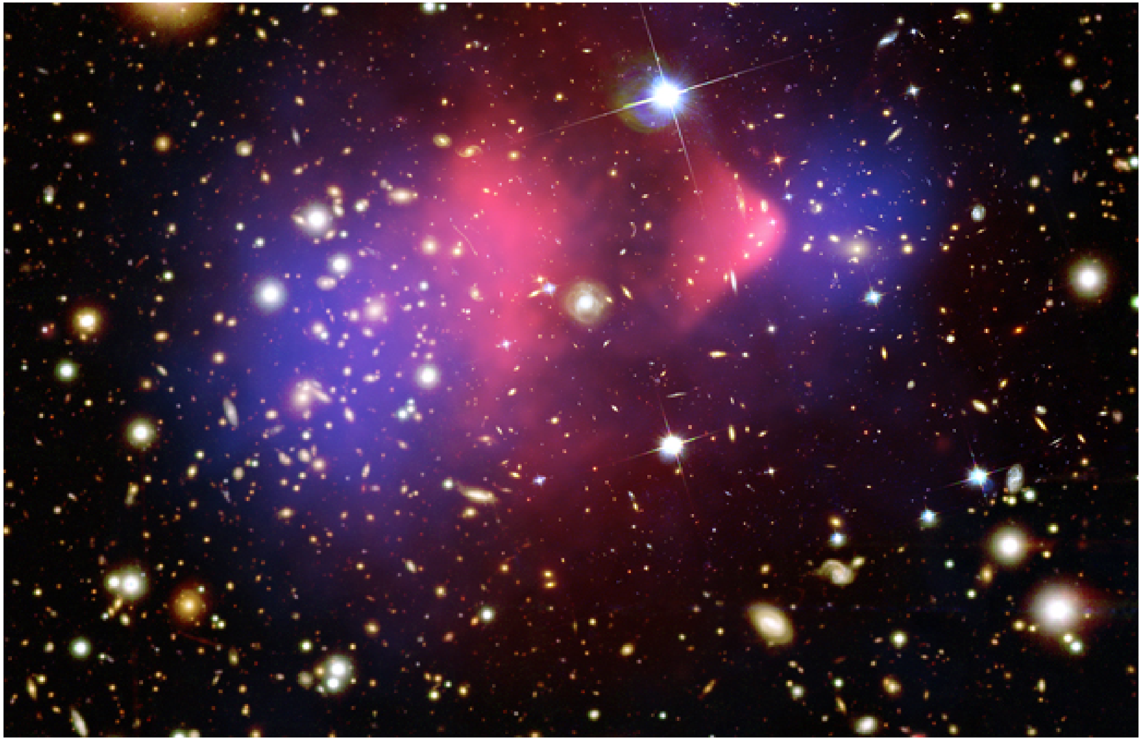

Bullet Cluster

Weak lensing:
A tool for tracing the large-scale distribution of matter

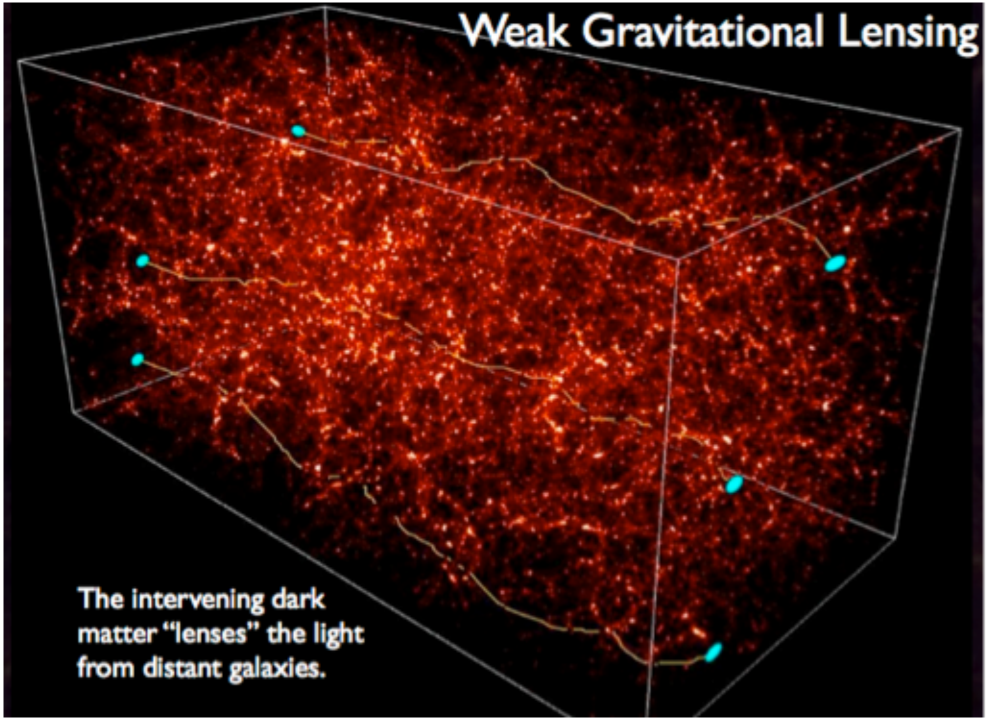

The cosmic web
S. Colombi and Y. Mellier (2014)

Microlensing:
A tool for detecting brown dwarfs, exoplanets etc.
B. Paczýnski (1986)

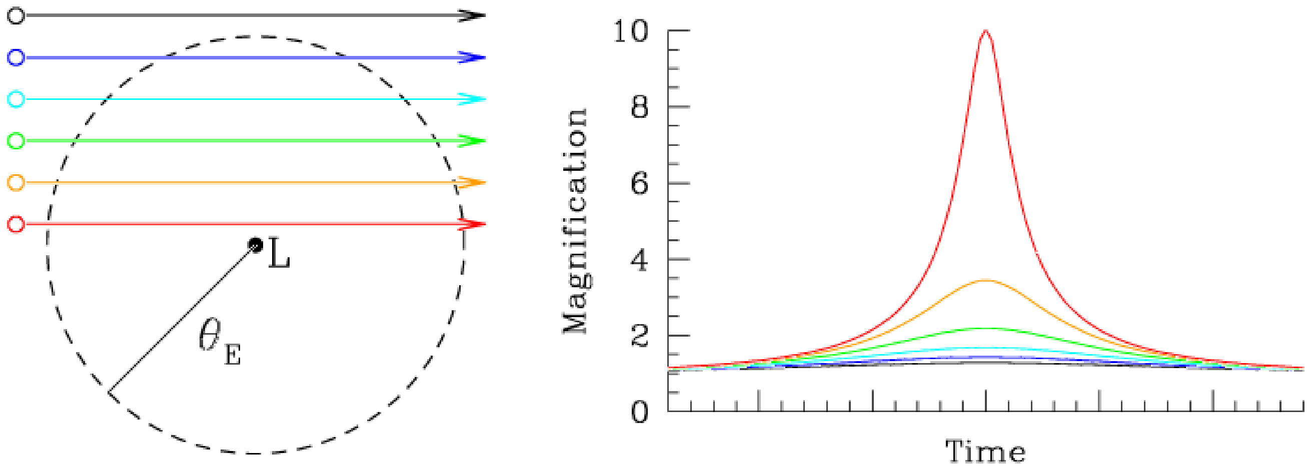

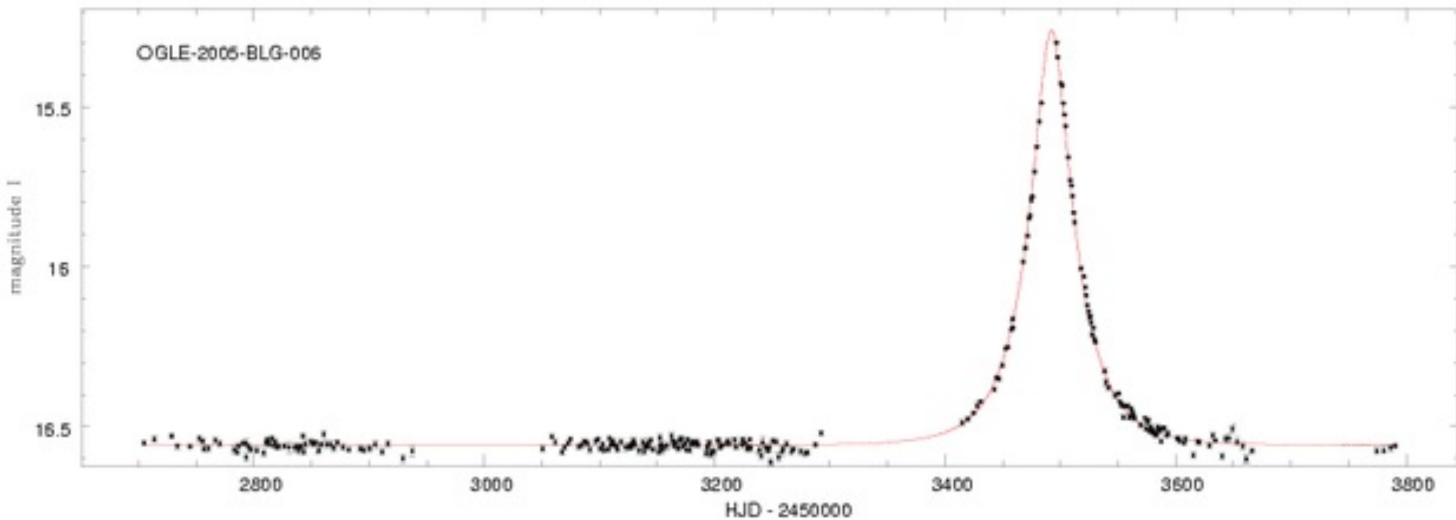
OGLE-2005-BLG-006
magnitude I
15.5
16
16.5
2800
3000
3200
3400
3600
3800
HJD - 2450000

Search for exoplanets

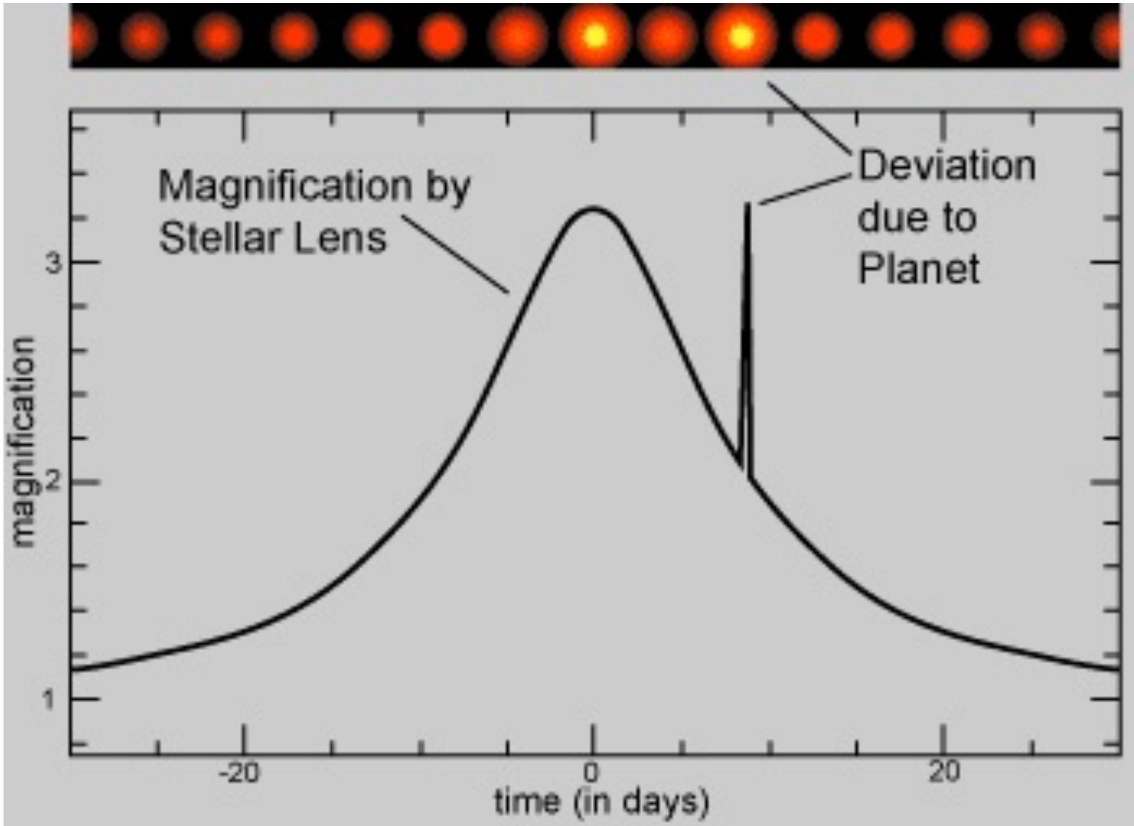

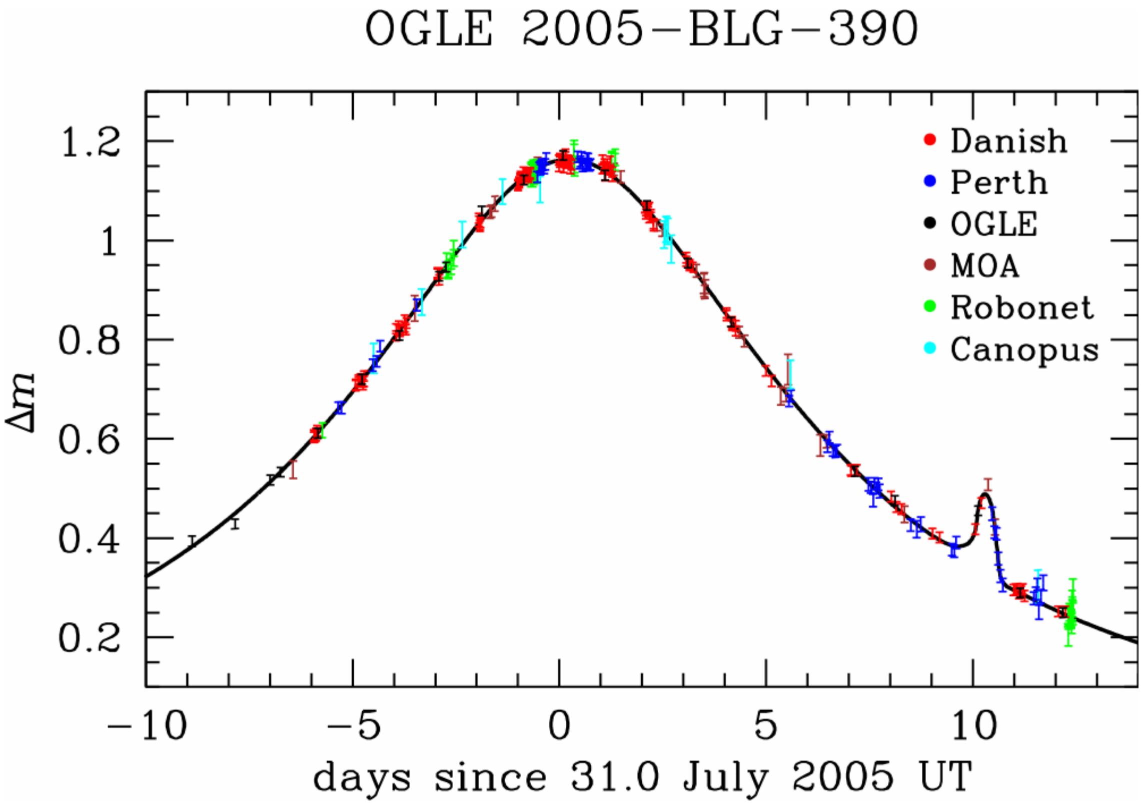

OGLE 2005−BLG−390
Danish
Perth
OGLE
MOA
Robonet
Canopus
1.2
1
0.8
0.6
0.4
0.2
Δm
−10
−5
0
5
10
days since 31.0 July 2005 UT

2. The weak-field formalism of lensing

S. Refsdal, 1964

Assumptions:

- Time-independent situation
- Deflecting mass concentrated in a plane
- Euclidean geometry valid outside of this plane

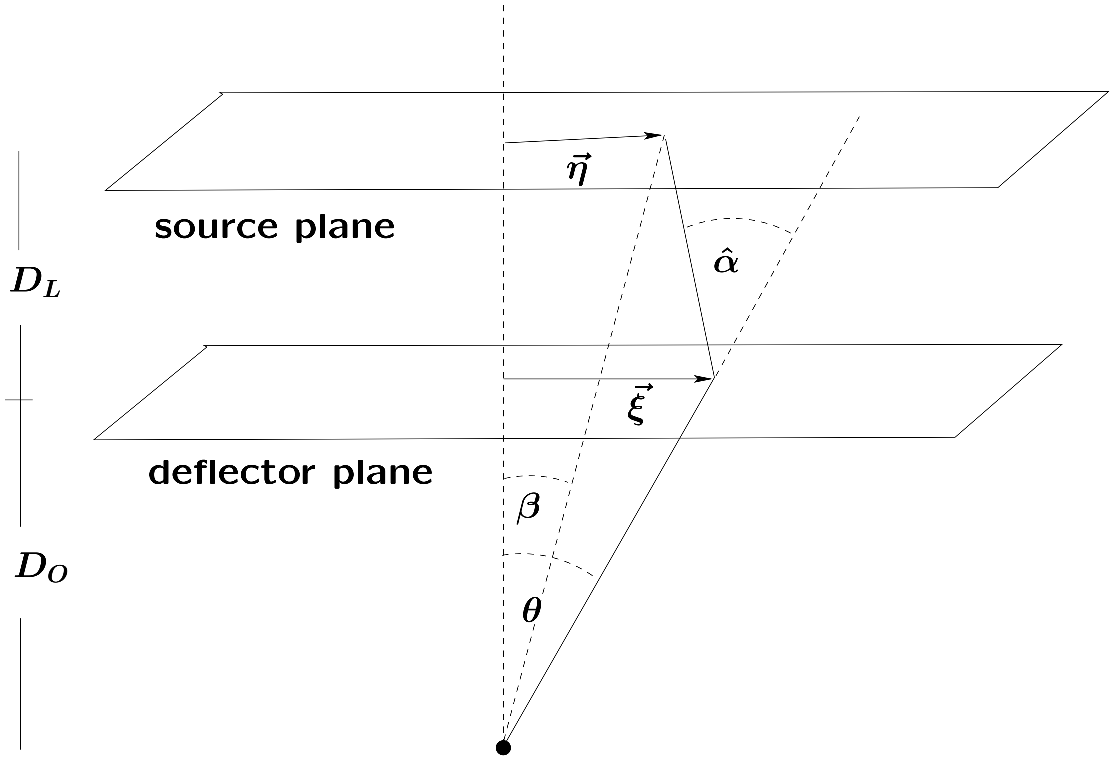

Lens map: deflector plane $\rightarrow$ source plane, $\vec{\xi} \mapsto \vec{\eta}$

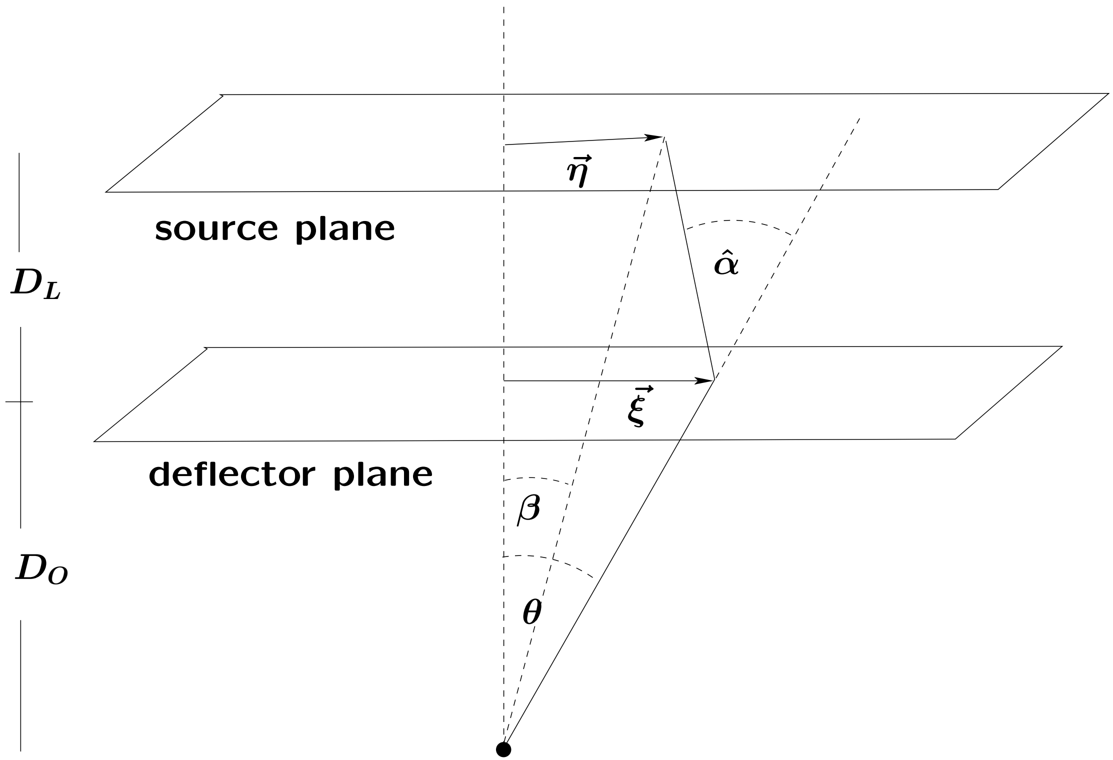

- **Angles β, θ and $\hat{\alpha}$ small**

Lens map $\vec{\xi} \mapsto \vec{\eta}$ given by lens equation

$$\vec{\eta} = \frac{D_L + D_O}{D_O}\,\vec{\xi} - D_L\,\vec{\hat{\alpha}}$$

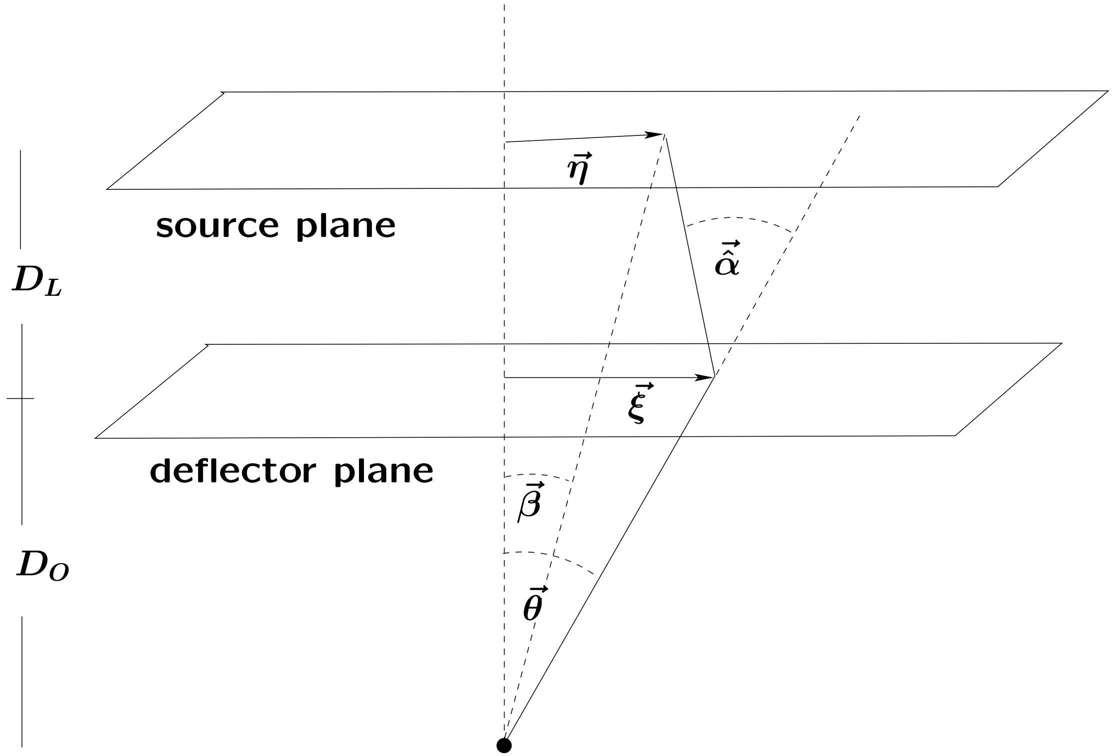

$$\underbrace{\frac{\vec{\eta}}{D_L + D_O}}_{=:\vec{\beta}} = \underbrace{\frac{\vec{\xi}}{D_O}}_{=:\vec{\theta}} - \underbrace{\frac{D_L}{D_L + D_O}\vec{\hat{\alpha}}}_{=:\vec{\alpha}}$$

lens equation in dimensionless form: $\vec{\beta} = \vec{\theta} - \vec{\alpha}$

Bending angle $\vec{\hat{\alpha}}$ is determined by two additional assumptions:

- For a point mass M at $\vec{\xi'}$ Einstein's formula holds

$$\vec{\hat{\alpha}} = \frac{4GM}{c^2} \frac{(\vec{\xi} - \vec{\xi'})}{|\vec{\xi} - \vec{\xi'}|^2}$$

- The superposition principle holds

Then, for a surface mass density $\Sigma(\vec{\xi'})$,

$$\vec{\hat{\alpha}} = \frac{4G}{c^2} \int_{\mathbb{R}^2} \frac{(\vec{\xi} - \vec{\xi'})}{|\vec{\xi} - \vec{\xi'}|^2} \Sigma(\vec{\xi'})\, d^2\vec{\xi'} = \begin{pmatrix} \dfrac{\partial V(\vec{\xi})}{\partial \xi_1} \\ \dfrac{\partial V(\vec{\xi})}{\partial \xi_2} \end{pmatrix}$$

where

$$V(\vec{\xi}) = \frac{4G}{c^2} \int_{\mathbb{R}^2} \Sigma(\vec{\xi'}) \ln|\vec{\xi} - \vec{\xi'}|\, d^2\vec{\xi'}$$

All lensing features are coded in the lens equation $\vec{\beta} = \vec{\theta} - \vec{\alpha}$:

- **Multiple imaging is determined by how many $\vec{\theta}_1, \ldots, \vec{\theta}_n$ are mapped by the lens equation onto the same $\vec{\beta}$.**
- **Brightness of images is given by the magnification μ,**

$$\mu^{-1} = \det\left(\frac{\partial\vec{\beta}}{\partial\vec{\theta}}\right)$$

Caustic points are characterised by $\mu = \infty$

Example: Point lens

$$\vec{\hat{\alpha}} = \frac{4GM}{c^2} \frac{\vec{\xi}}{\left|\vec{\xi}\right|^2}$$

$$\vec{\beta} = \vec{\theta} - \frac{D_L}{(D_L + D_O)} \frac{4GM}{c^2} \frac{\vec{\theta}}{D_O \left|\vec{\theta}\right|^2}$$

With $\vec{\beta} = \beta\,\vec{e}$ **and** $\vec{\theta} = \theta\,\vec{e}$**:**

$$\beta = \theta - \frac{4GMD_L}{c^2(D_L + D_O)\,D_O} \frac{1}{\theta}$$

Einstein ring $\left(\beta = 0\right)$ occurs at $\theta_E = \sqrt{\dfrac{4GMD_L}{c^2\left(D_O + D_L\right) D_O}}$

Lens equation can be written as

$$\beta = \theta - \frac{\theta_E^2}{\theta}$$

Two solutions for each $\beta > 0$,

$$\theta_\pm = \frac{\beta}{2} \pm \sqrt{\frac{\beta^2}{4} + \theta_E^2}$$

i.e., there is double-imaging

Magnification

$$\mu_\pm = \frac{1}{1 - \dfrac{\theta_E^4}{\theta_\pm^4}} = \frac{\pm\left(\beta \pm \sqrt{\beta^2 + 4\,\theta_E^2}\right)^2}{4\,\beta\sqrt{\beta^2 + 4\,\theta_E^2}}$$

Calculate micro-lensing light curve for source moving in a straight line:

$$\beta = \sqrt{\beta_1^2 + \beta_2^2}$$

$$\beta_1 = \theta_E \frac{t}{t_E}$$

$$\beta_2 = \theta_E \, u_m$$

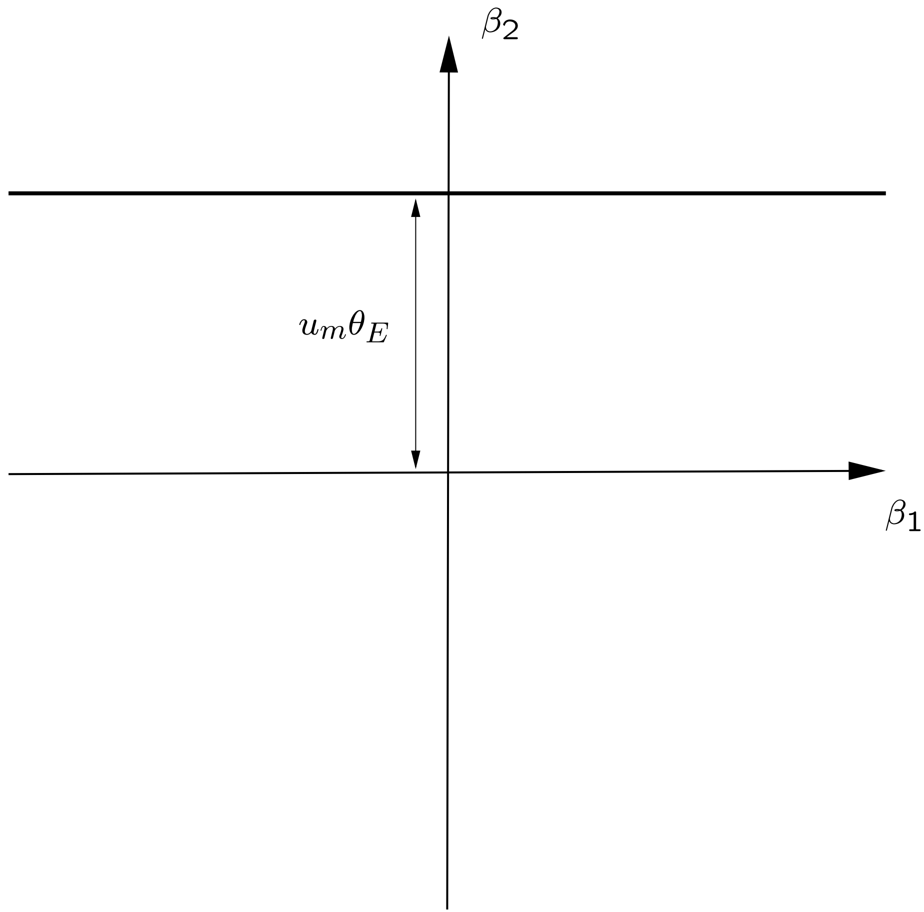

Total magnification:

$$\mu = |\mu_+| + |\mu_-| = \frac{u_m^2 + \frac{t^2}{t_E^2} + 2}{\sqrt{u_m^2 + \frac{t^2}{t_E^2}}\sqrt{u_m^2 + \frac{t^2}{t_E^2} + 4}}$$

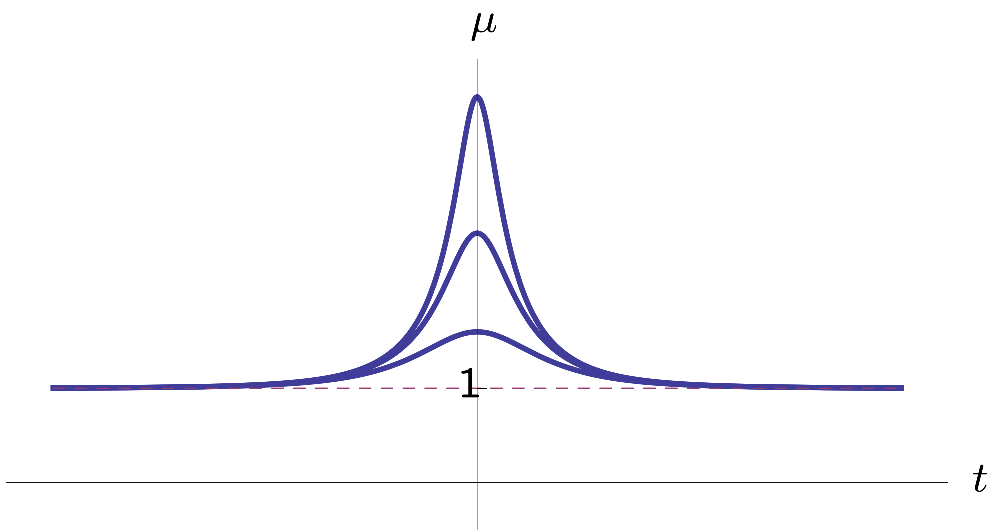

3. Schwarzschild lensing and generalisations

metrics

Schwarzschild metric:

$$g_{\mu\nu}dx^\mu dx^\nu = -\left(1-\frac{2m}{r}\right)c^2dt^2 + \frac{dr^2}{1-\dfrac{2m}{r}} + r^2\left(d\vartheta^2 + \sin^2\vartheta\, d\varphi^2\right)$$

$$m = \frac{GM}{c^2}$$

Lightlike geodesics in the equatorial plane:

$$\left(\frac{dr}{d\varphi}\right)^2 = \frac{c^2E^2r^4}{L^2} - r^2\left(1-\frac{2m}{r}\right)$$

E,L: constants of motion

Deflection angle:

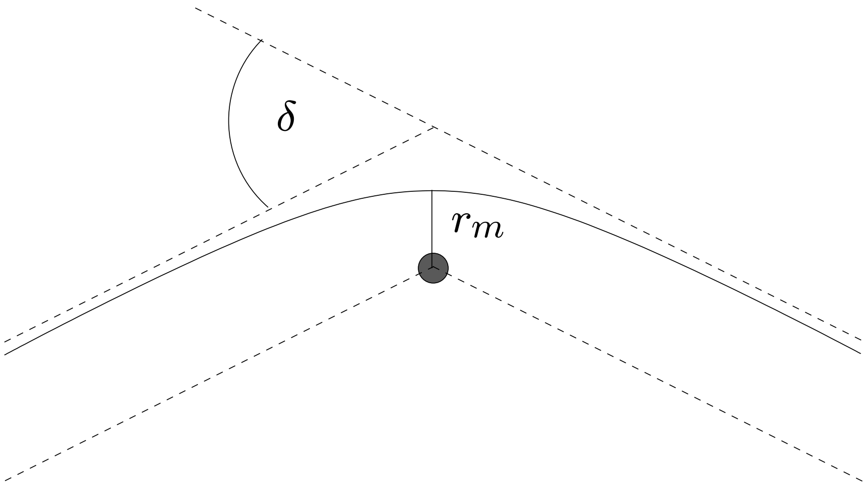

$$\left.\frac{dr}{d\varphi}\right|_{r_m} = 0 \implies$$

$$\frac{c^2 E^2}{L^2} = \frac{1}{r_m^2} - \frac{2m}{r_m^3}$$

$$\pi + \delta = 2 \int_{r_m}^{\infty} \frac{r_m \, dr}{\sqrt{\left(1 - \frac{r_S}{r_m}\right) r^4 - r_m^2 \, r^2 + r_m^2 \, r_S \, r}}$$

$$\delta = \frac{4m}{r_m} + \dots$$

Circular lightlike geodesics:

$$\frac{dr}{d\varphi} = 0\,, \qquad \frac{d^2r}{d\varphi^2} = 0 \qquad \Longrightarrow \qquad \frac{L^2}{E^2} = 27\,c^2\,m^2\,, \qquad r = 3m$$

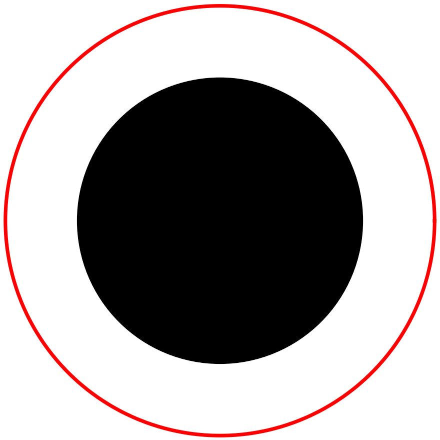

Horizon:

$r = r_S = 2m$

Light sphere (photon sphere):

$r = r_p = 3m$

Circular lightlike geodesics (unstable):

$$\frac{dr}{d\varphi} = 0\,, \quad \frac{d^2r}{d\varphi^2} = 0 \quad \Longrightarrow \quad \frac{L^2}{E^2} = 27\,c^2\,m^2\,, \quad r = 3m$$

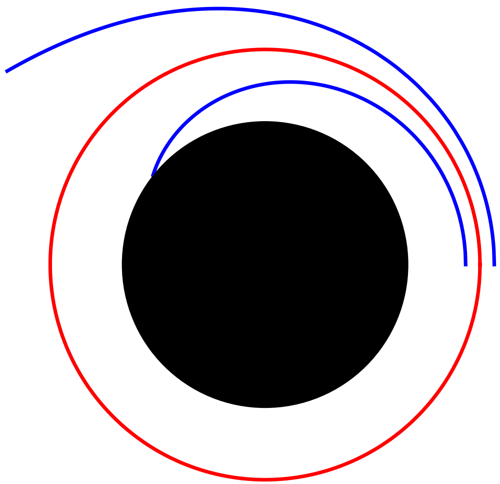

Horizon:

$r = r_S = 2m$

Light sphere (photon sphere):

$r = r_p = 3m$

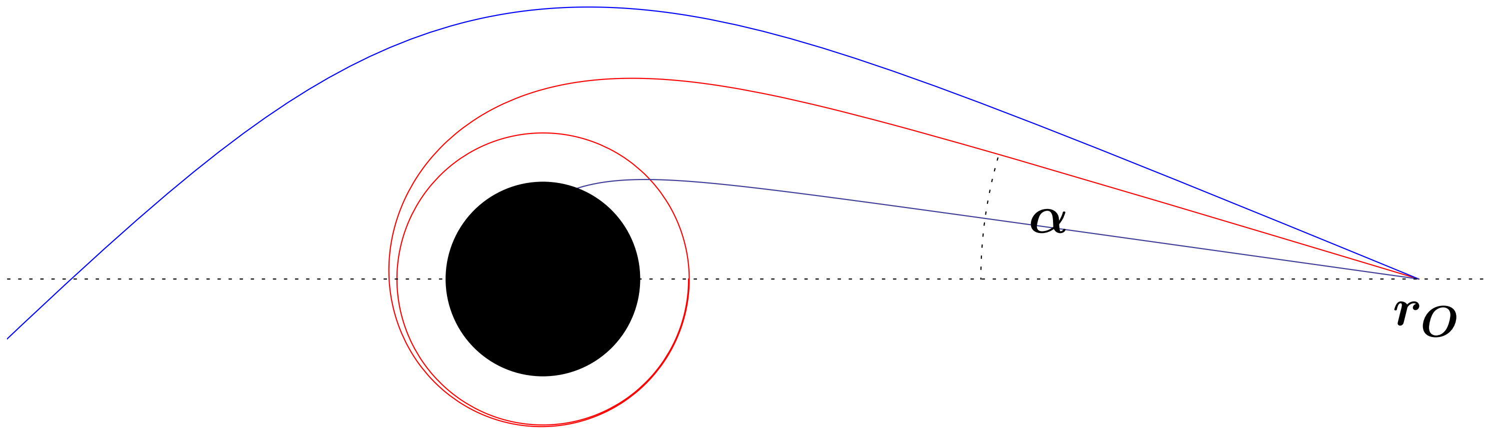

Angular radius α of the "shadow" of a Schwarzschild black hole:

$$\sin^2\alpha = \frac{27\, m^2}{r_O^2}\Big(1 - \frac{2m}{r_O}\Big)$$

J. L. Synge, Mon. Not. R. Astr. Soc. 131, 463 (1966)

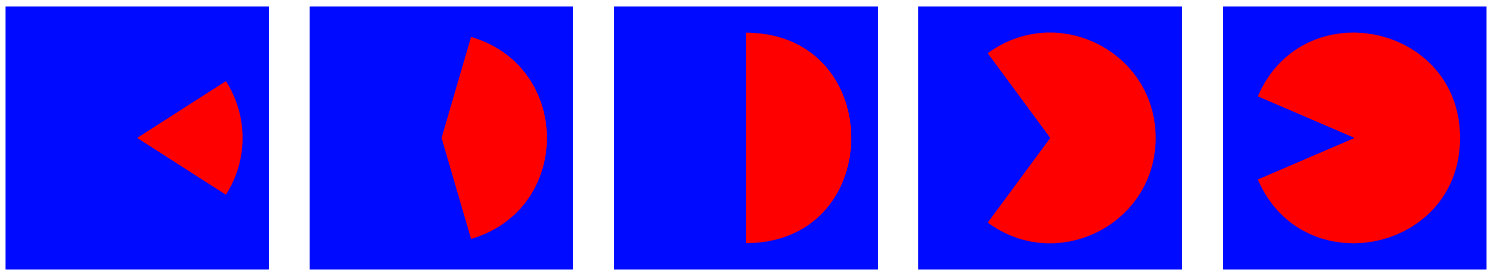

$r_O = 1.05\, r_S$ $\quad$ $r_O = 1.3\, r_S$ $\quad$ $r_O = 3\, r_S/2$ $\quad$ $r_O = 2.5\, r_S$ $\quad$ $r_O = 6\, r_S$

Schwarzschild black hole produces infinitely many images:

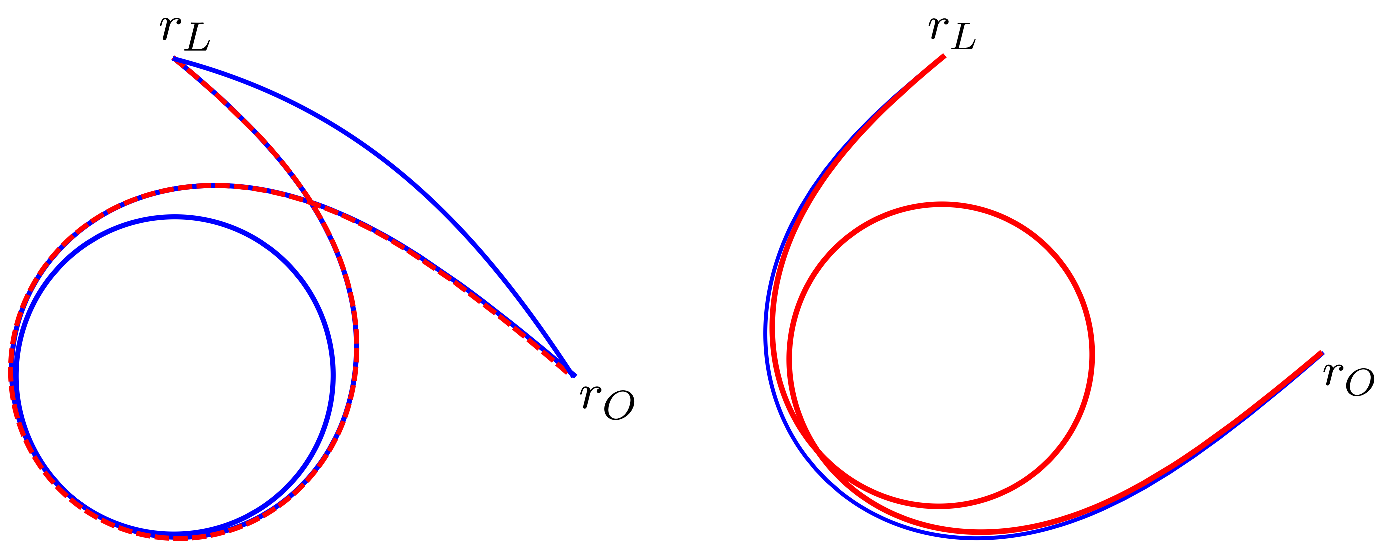

Visual appearance of a Schwarzschild black hole

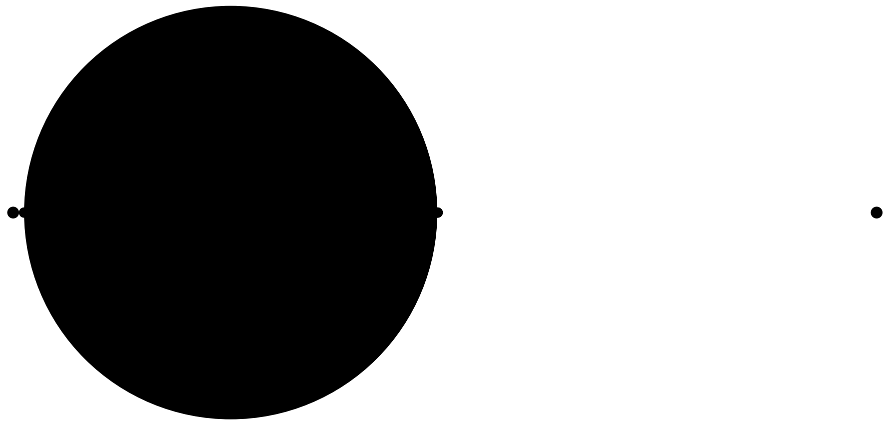

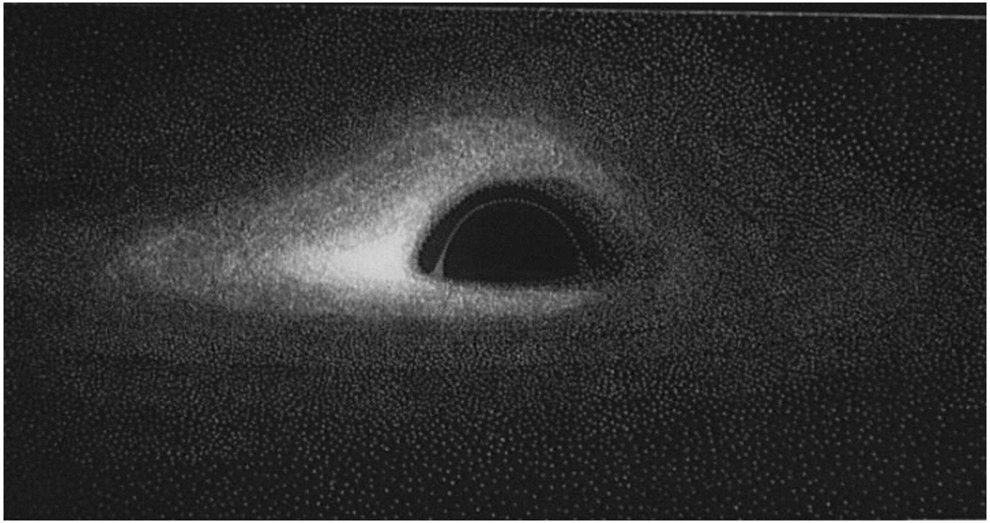

J.-P. Luminet (1979)

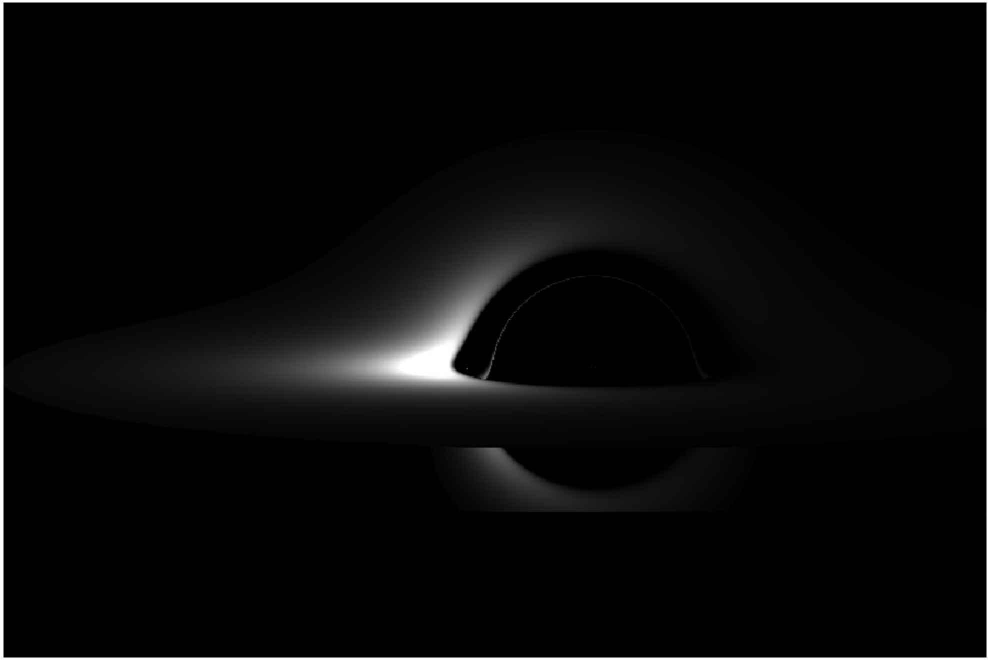

T. Müller (2012)

Perspectives of observations

Object at the centre of our galaxy:

Mass $= 4.3 \times 10^6 \, M_\odot$

Distance $= 8.3 \, \mathrm{kpc}$

Synge's formula gives for the diameter of the shadow $\approx 54\mu$as

(corresponds to a grapefruit on the moon)

Object at the centre of M87:

Mass $= 3 \times 10^9 \, M_\odot$

Distance $= 16 \, \mathrm{Mpc}$

Synge's formula gives for the diameter of the shadow $\approx 20\mu$as

Project to view the shadow with (sub-)millimeter VLBI:

Event Horizon Telescope (EHT),

Using ALMA, NOEMA, LMT, SMT, SPT ...

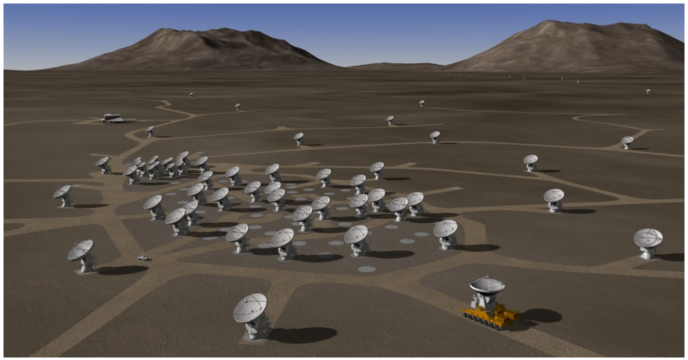

ALMA

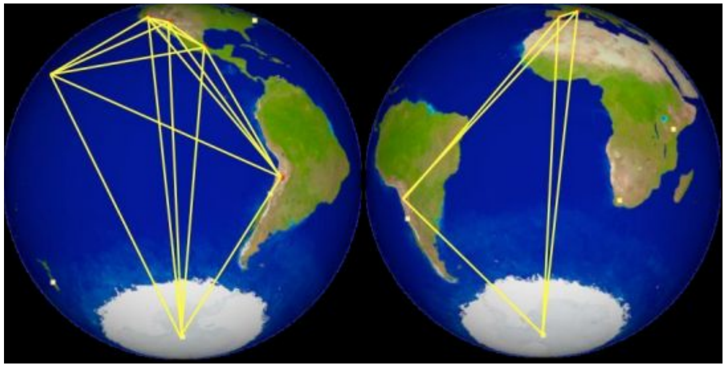

EHT

Announcement of results expected ca. for January 2019 no scattering   scattering, $0.6\,\mathrm{mm}$ scattering, $1.3\,\mathrm{mm}$

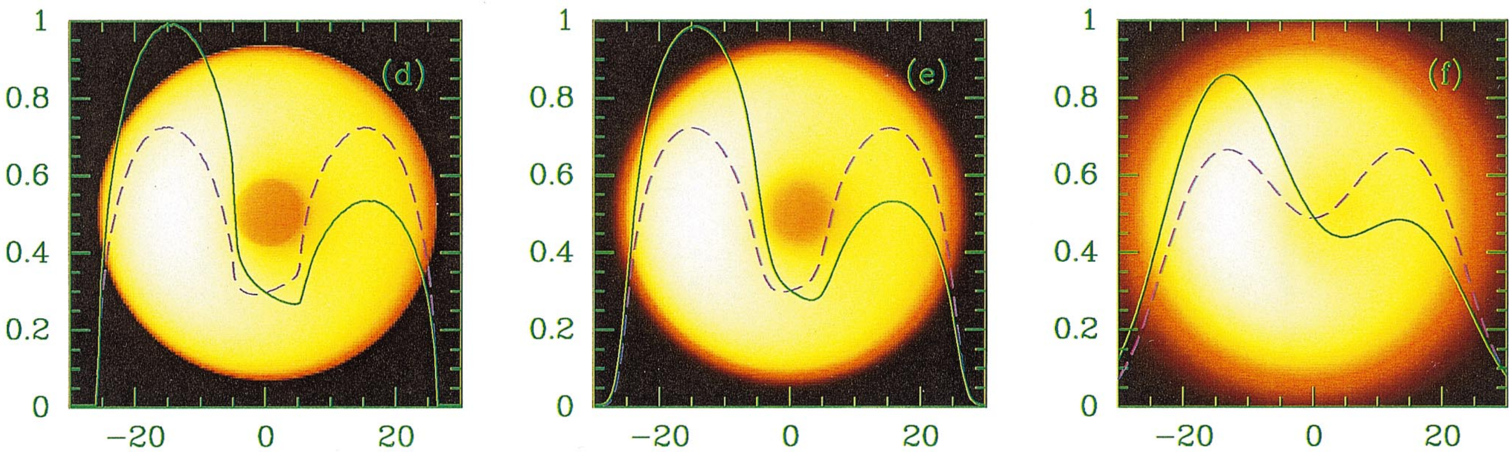

From H. Falcke, F. Melia and E. Agol:
Astrophys. J. 528, L13 (2000)

The observation of the shadow is NOT an ultimate proof that there is a black hole!

Black hole impostor: Ultracompact star

Dark star with radius between $2m$ and $3m$

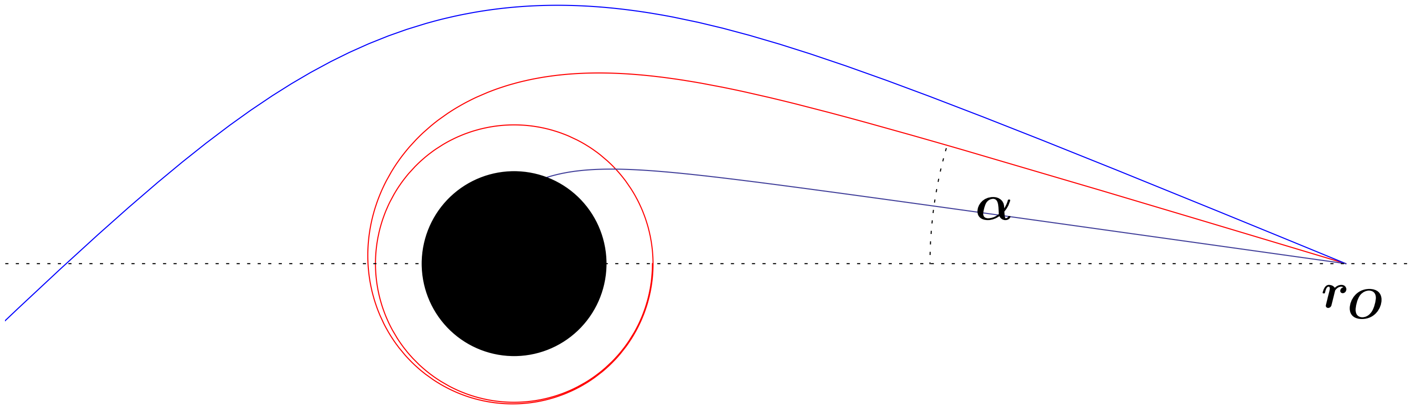

Shadow indistinguishable from Schwarzschild black hole

Ultracompact objects are unstable, see

V. Cardoso, L. Crispino, C. Macedo, H. Okawa, P. Pani:
Phys. Rev. D 90, 044069 (2014)

Black hole impostor: Ellis wormhole

H. Ellis: J. Math. Phys. 14, 104 (1973)

$$g_{\mu\nu}dx^{\mu}dx^{\nu} = -c^2dt^2 + dr^2 + \left(r^2 + a^2\right)\left(d\vartheta^2 + \sin^2\vartheta\, d\varphi^2\right)$$

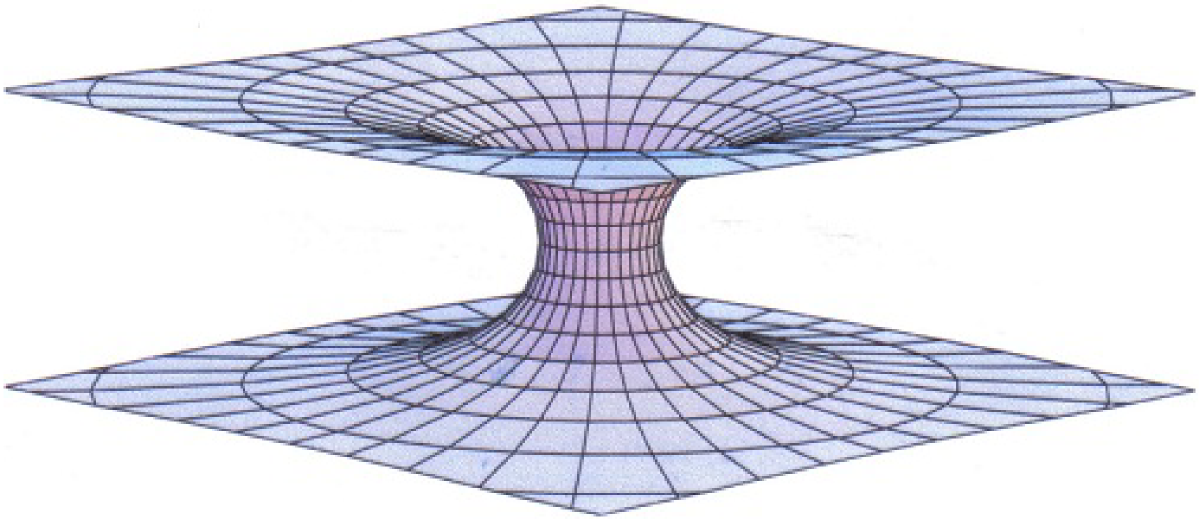

Angular radius α of shadow: $\sin^2\alpha = \dfrac{a^2}{r_O^2 + a^2}$

Exact lens map for spherically symmetric and static metrics [VP: Phys. Rev. D 69, 064917 (2004)]

$$g_{\mu\nu}dx^{\mu}dx^{\nu} = e^{2f(r)}\Big(-c^2dt^2 + S(r)^2dr^2 + R(r)^2\big(d\vartheta^2 + \sin^2\vartheta\, d\varphi^2\big)\Big)$$

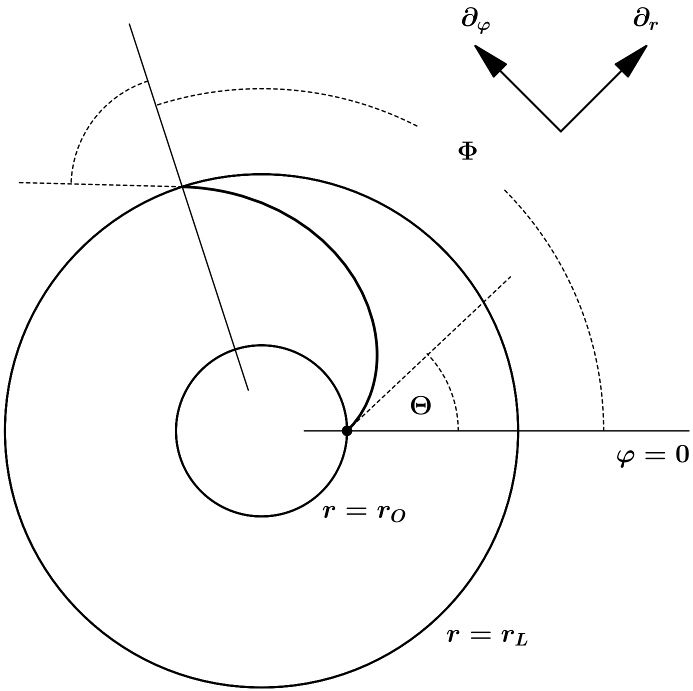

$$\Phi \;=\; R(r_O)\sin\Theta \int_{r_O}^{r_L} \frac{S(r)\,dr}{R(r)\sqrt{R(r)^2 \,-\, R(r_O)^2\sin^2\Theta}}$$

Example 1: Schwarzschild spacetime:

$$S(r) = \left(1 - \frac{2m}{r}\right)^{-1}, \qquad R(r) = \frac{r}{\sqrt{1 - \frac{2m}{r}}}$$

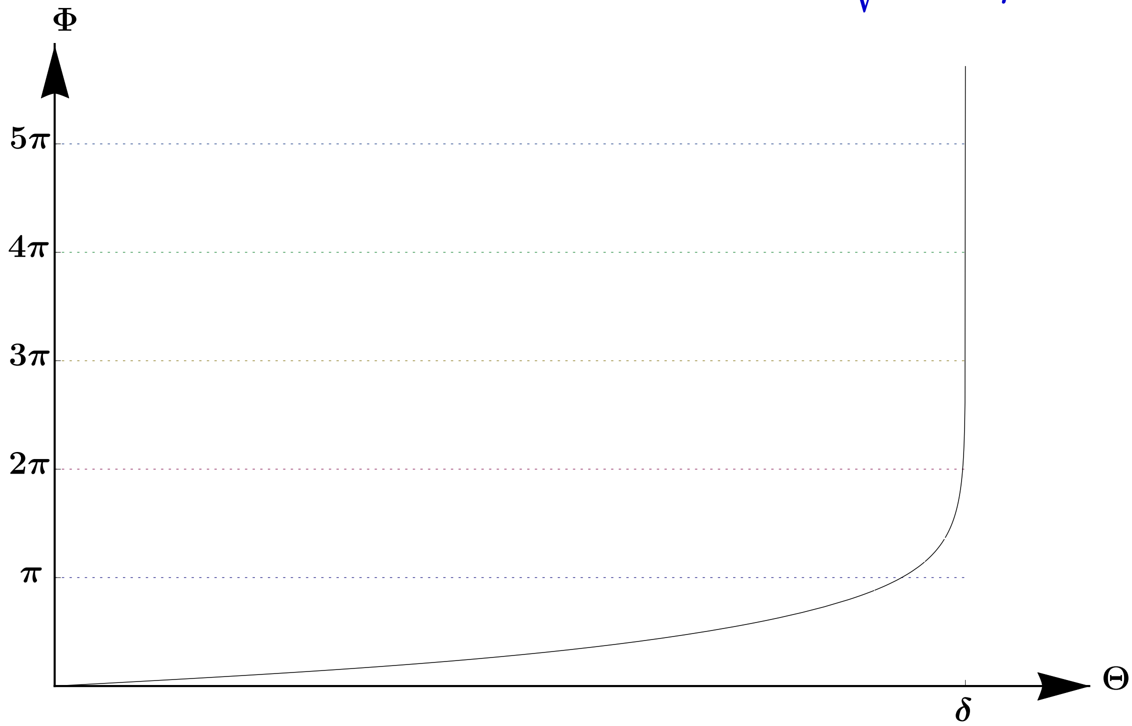

Lens map $\Theta \mapsto \Phi$ for $2m < r_O < r_L$

Infinite sequence of images converges towards boundary of the shadow

Example 2: Ellis wormhole:

$$S(r) = 1 \,, \qquad R(r) = \sqrt{a^2 + r^2}$$

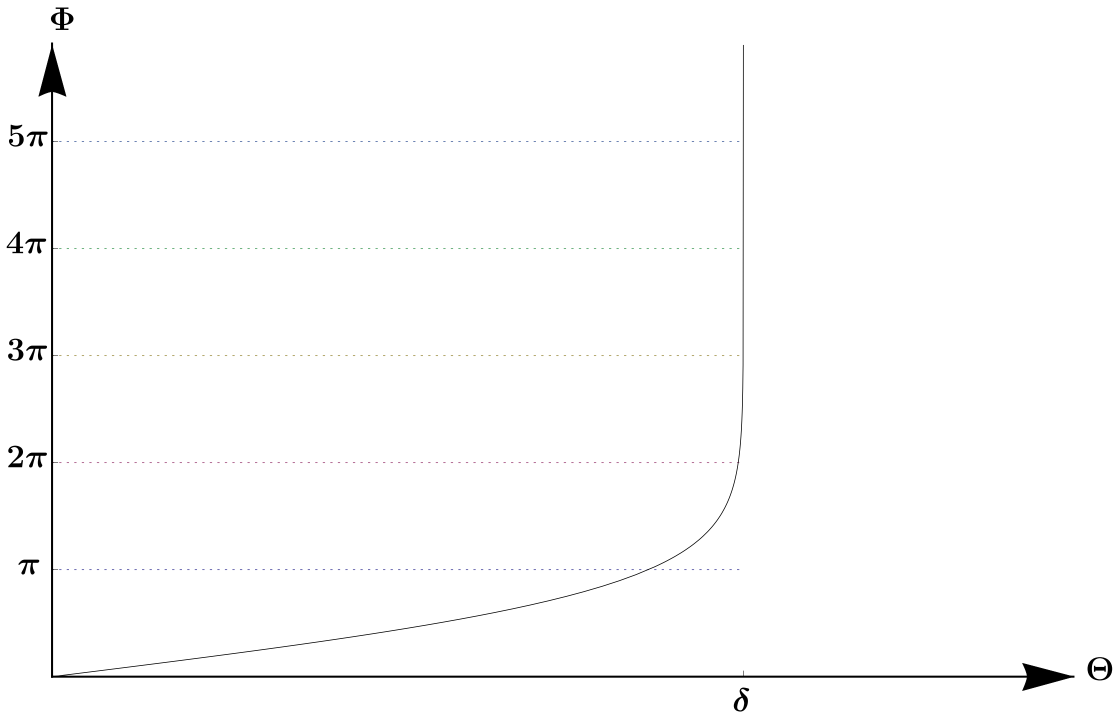

Lens map $\Theta \mapsto \Phi$ for $-\infty < r_O < r_L$

Infinite sequence of images converges towards boundary of the shadow

Example 3: Barriola-Vilenkin monopole
M. Barriola, A. Vilenkin: Phys. Rev. Lett. 63, 341 (1989)

$$g_{\mu\nu}dx^\mu dx^\nu = -c^2dt^2 + dr^2 + k^2 r^2 \left(d\vartheta^2 + \sin^2\vartheta \, d\varphi^2 \right)$$

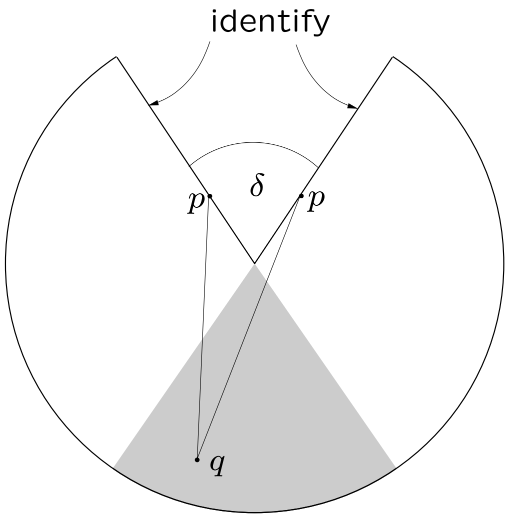

,

Such monopoles

- are approximate solutions to Einstein's field equation with a triplet of scalar fields as the source
- may have formed during a phase transition in the early universe

Lens map for the Barriola-Vilenkin monopole:

$$S(r) = 1\,, \quad R(r) = k\,r$$

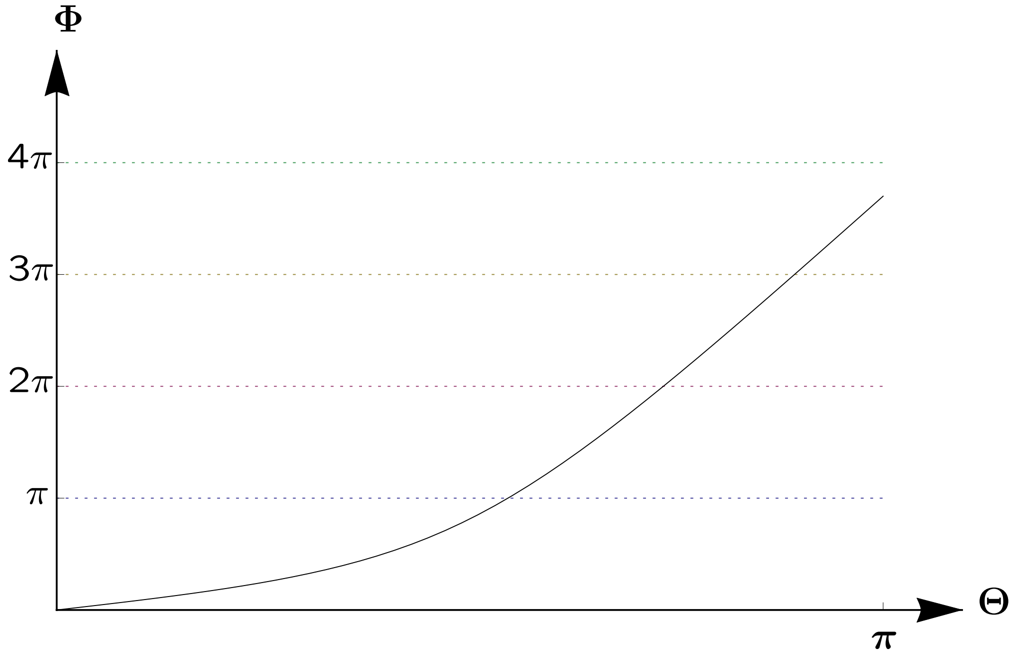

Lens map $\Theta \mapsto \Phi$ for $r_O < r_L$

Finitely many images, no shadow

Microlensing by a Barriola-Vilenkin monopole:

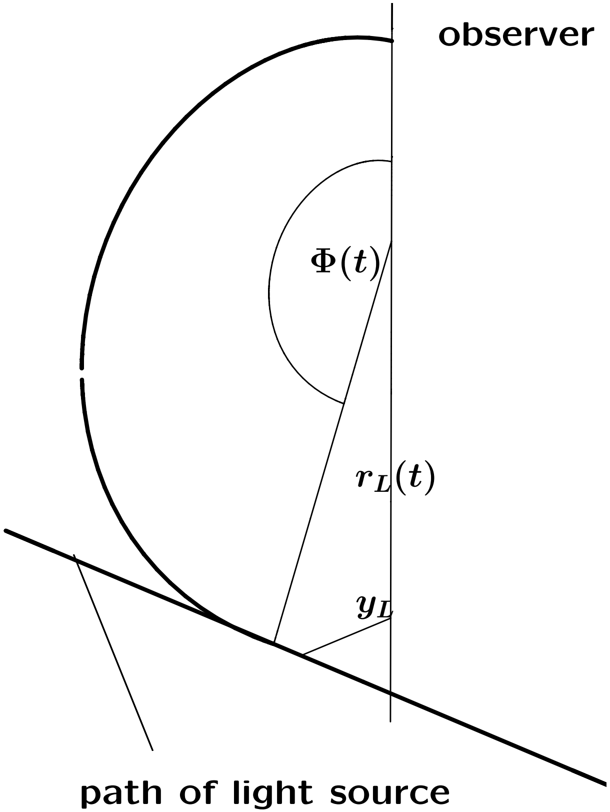

$$\begin{pmatrix} x(t) \\ y(t) \\ z(t) \end{pmatrix} = \begin{pmatrix} v\,t \\ y_L \\ z_L \end{pmatrix}$$

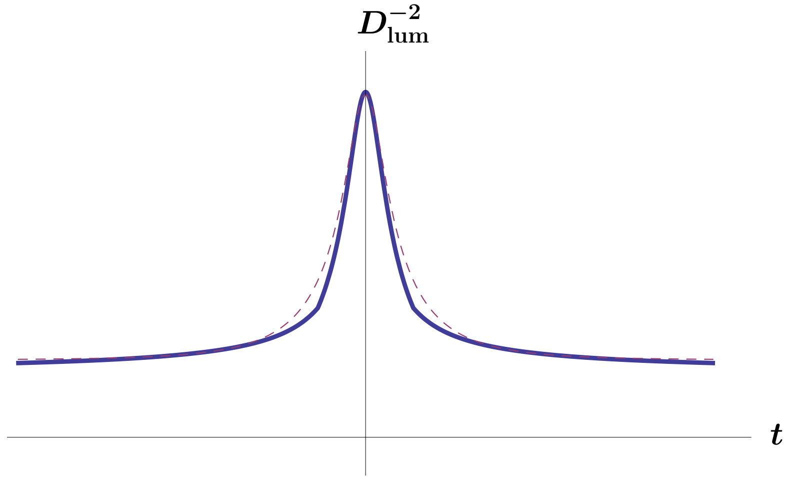

Other spherically symmetric and static metrics:

- Reissner-Nordström
- Kottler
- Janis-Newman-Winicour
- Black holes from nonlinear electrodynamics
- Black holes from Hořava-Lifshitz theories
- Black holes from $f(R)$ theories
- Black holes from Horndeski theories
- Black holes from higher dimensions
- Black holes from braneworld scenarios , $\ldots$

All of them have an unstable photon sphere (for some values of their parameters) $\Longrightarrow$ Qualitative lensing features are similar to Schwarzschild

Quantitative features (ratio of angular separations of images, ratio of fluxes of images) are different, see V. Bozza: Phys. Rev. D 66, 103001 (2002)

The shadow is always circular. Its angular radius depends on r_O and the parameters of the black hole.

Analytic formulas for the shadow in a plasma

Arbitrary spherically symmetric and static metric:

VP, O. Yu. Tsupko, G. S. Bisnovatyi-Kogan:
Phys. Rev. D 92, 104031 (2015)

So far: only pressureless ("cold") and non-magnetised plasmas have been considered

Hamilton formalism for light rays:

$$H(x,p) = \frac{1}{2}\Big(g^{\mu\nu} p_\mu p_\nu + \omega_p(x)^2 \Big)$$

For derivation of Hamiltonian see e.g. VP: "Ray optics, Fermat's principle and applications to general relativity" Springer (2000)

Example:

Schwarzschild spacetime

plasma frequency: $\omega_p(r)^2 = \beta_0\, \omega_0^2 \Big(\dfrac{m}{r} \Big)^{3/2}$

$a : r_O = 3.3\, m$

$b : r_O = 3.8\, m$

$c : r_O = 5\, m$

$d : r_O = 10\, m$

$e : r_O = 50\, m$

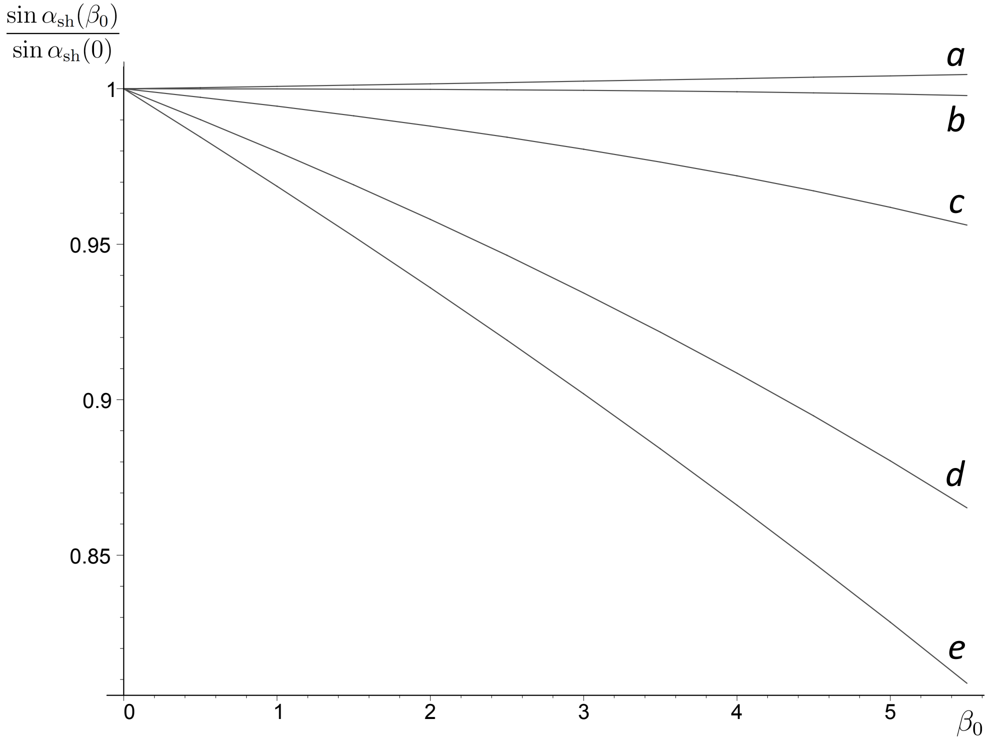

4. Kerr lensing and generalisations to other non-static metrics

Shadow no longer circular

Shape of shadow can be used for discriminating between different black holes

Shape of the shadow of a Kerr black hole for observer at infinity:

J. Bardeen in C. DeWitt and B. DeWitt (eds.): “Black holes” Gordon & Breach (1973)

Shape and size of the shadow for black holes of the Plebański-Demiański class for observer at coordinates (r_O, ϑ_O) (analytical formulas):

A. Grenzebach, VP, C. Lämmerzahl: Phys. Rev. D 89, 124004 (2014), Int. J. Mod. Phys. D 24, 1542024 (2015)

A. Grenzebach: “The shadow of black holes. An analytic description.” Springer Briefs in Physics, Springer, Heidelberg (2016)

Kerr metric in Boyer–Lindquist coordinates $(r, \vartheta, \varphi, t)$:

$$g_{\mu\nu}dx^\mu dx^\nu = \varrho(r,\vartheta)^2 \left(\frac{dr^2}{\Delta(r)} + d\vartheta^2 \right) + \frac{\sin^2\vartheta}{\varrho(r,\vartheta)^2} \Big(a\, dt - (r^2 + a^2) d\varphi \Big)^2$$

$$- \frac{\Delta(r)}{\varrho(r,\vartheta)^2} \Big(dt - a \sin^2\!\vartheta\, d\varphi \Big)^2$$

$$\varrho(r,\vartheta)^2 = r^2 + a^2 \cos^2\vartheta, \qquad \Delta(r) = r^2 - 2mr + a^2 \,.$$

$m = \dfrac{GM}{c^2}$ where M =mass , $\quad a = \dfrac{J}{Mc}$ where J =spin

Plebański-Demiański black holes: Additional parameters

q_e = el. charge , q_m = magn. charge , ℓ = NUT parameter ,

Λ = cosmol. constant , α = acceleration

Consider in the following only the Kerr metric

Lightlike geodesics:

$$\varrho(r,\vartheta)^2\dot{t} = a\left(L - Ea\,\sin^2\vartheta\right) + \frac{(r^2+a^2)\left((r^2+a^2)E - aL\right)}{\Delta(r)},$$

$$\varrho(r,\vartheta)^2\dot{\varphi} = \frac{L - Ea\,\sin^2\vartheta}{\sin^2\vartheta} + \frac{(r^2+a^2)aE - a^2L}{\Delta(r)},$$

$$\varrho(r,\vartheta)^4\dot{\vartheta}^2 = K - \frac{(L - Ea\,\sin^2\vartheta)^2}{\sin^2\vartheta} =: \Theta(\vartheta),$$

$$\varrho(r,\vartheta)^4\dot{r}^2 = -K\Delta(r) + \left((r^2+a^2)E - aL\right)^2 =: R(r).$$

Spherical lightlike geodesics exist in the region where

$$R(r) = 0\,, \quad R'(r) = 0\,, \quad \Theta(\vartheta) \geq 0\,.$$

$$\left(2r\Delta(r) - (r-m)\,\varrho(r,\vartheta)^2\right)^2 \leq 4a^2r^2\Delta(r)\,\sin^2\vartheta$$

(unstable if $R''(r) \geq 0$)

Photon region for Kerr black hole with $a = 0.75\,m$

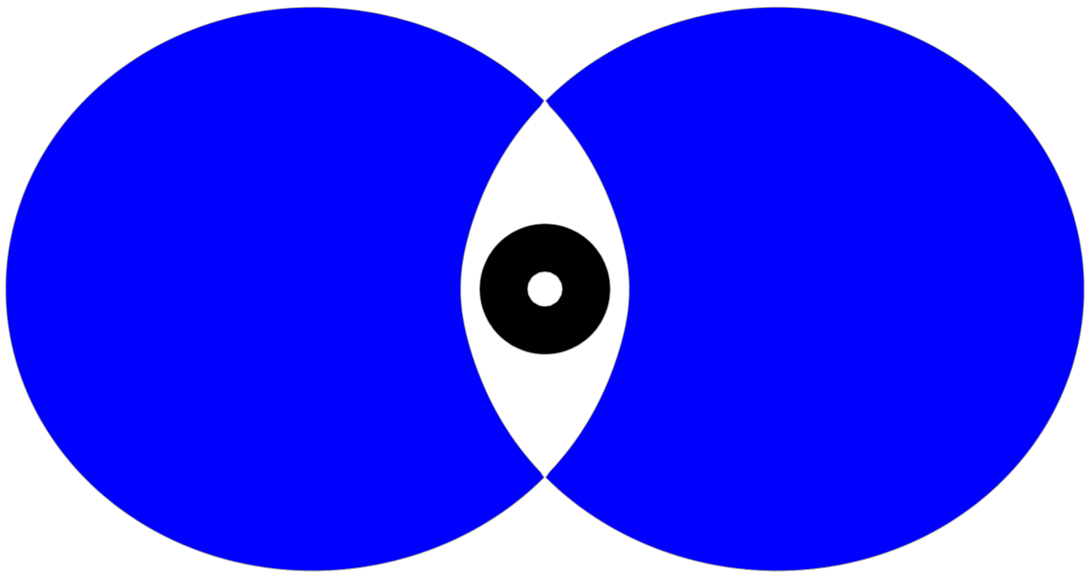

Photon region for Kerr black hole with $a = 0.75\, m$

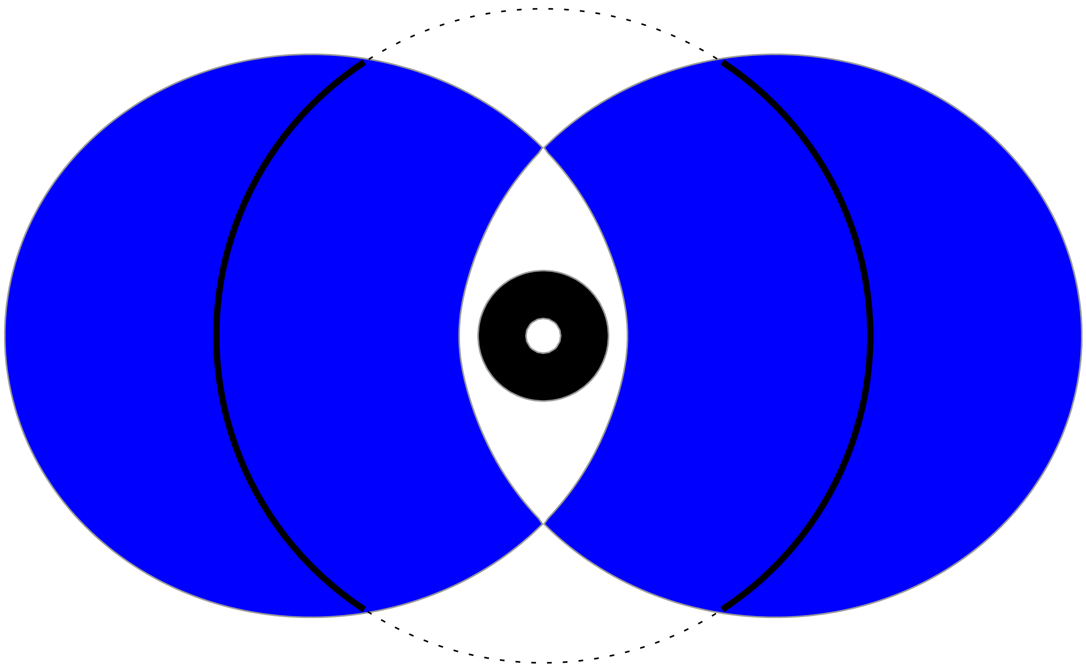

Photon region for Kerr black hole with $a = 0.75\,m$

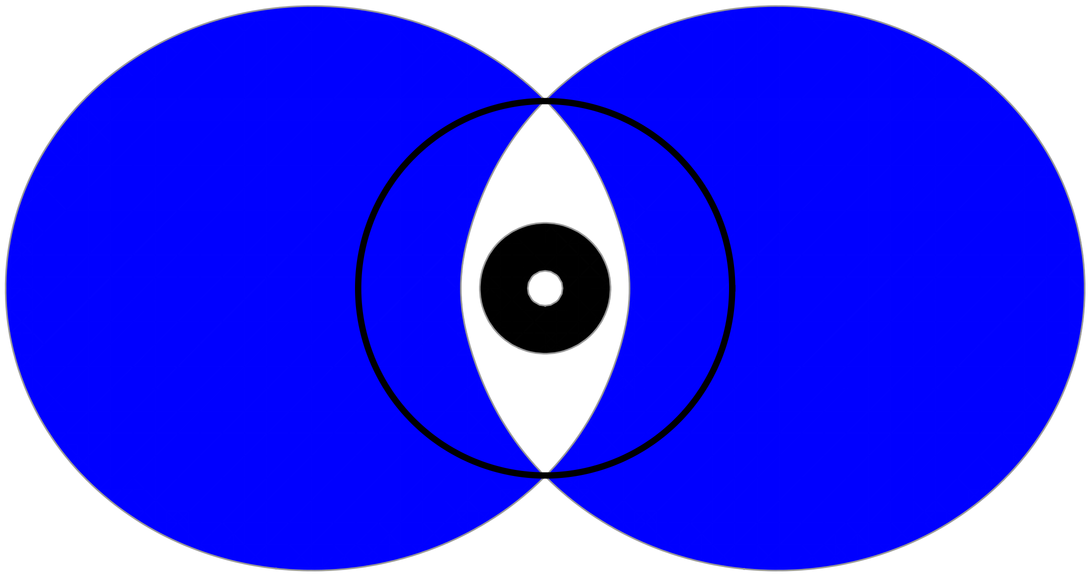

Photon region for Kerr black hole with $a = 0.75\,m$

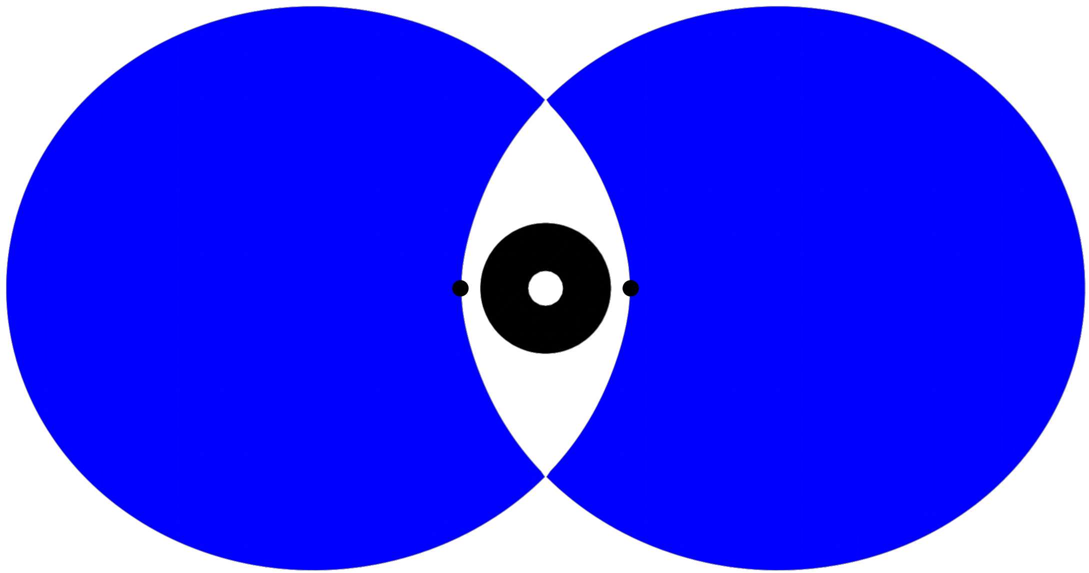

Photon region for Kerr black hole with $a = 0.75\,m$

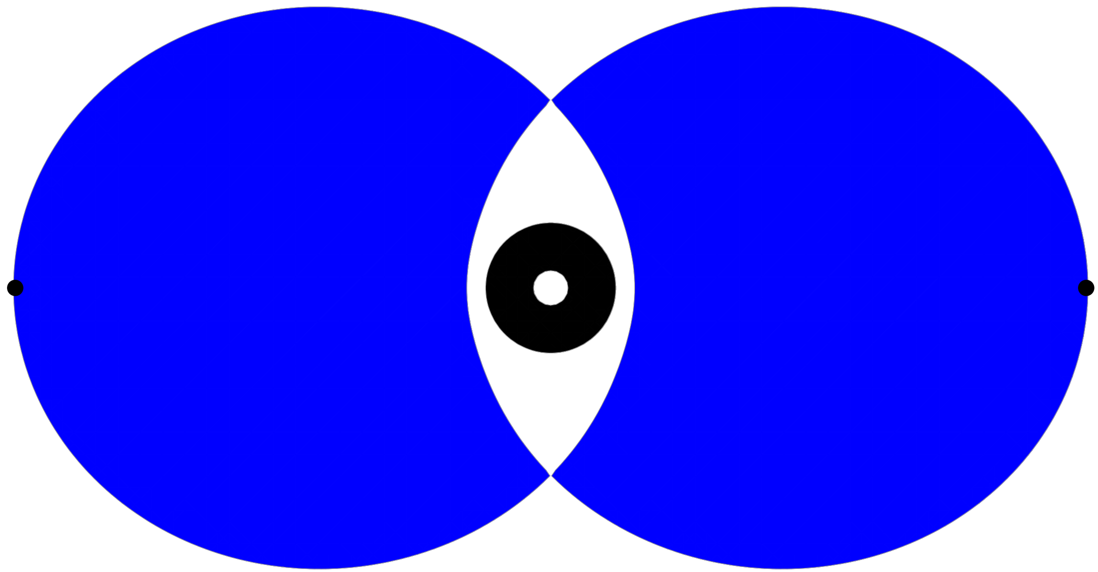

The shadow is determined by light rays that approach an unstable spherical lightlike geodesic.

Relation between constants of motion $\left(K_E = \dfrac{K}{E^2}, L_E = \dfrac{L}{E} - a\right)$ and celestial coordinates (θ, ψ):

$$\sin\theta = \frac{\sqrt{\Delta(r)\ K_E}}{r^2 - aL_E}\bigg|_{r=r_O}, \qquad \sin\psi = \frac{L_E + a\cos^2\vartheta + 2\ell\cos\vartheta}{\sqrt{K_E}\ \sin\vartheta}\bigg|_{\vartheta=\vartheta_O}$$

Constants of motion $\left(K_E, L_E\right)$ for limiting spherical lightlike geodesics:

$$K_E = \frac{16r^2\Delta(r)}{(\Delta'(r))^2}\bigg|_{r=r_p}, \qquad aL_E = \left(r^2 - \frac{4r\Delta(r)}{\Delta'(r)}\right)\bigg|_{r=r_p}$$

Gives boundary curve of the shadow $\theta(r_p), \psi(r_p)$ parametrised with r_p

Analytic formula for shadow allows to extract parameters of the spacetime from the shape of the shadow

Vertical angular radius α_v of the shadow ($\vartheta = \pi/2$)

$$\sin^2 \alpha_v = \frac{27m^2 r_O^2 \big(a^2 + r_O(r_O - 2m)\big)}{r_O^6 + 6a^2 r_O^4 + 3a^2(4a^2 - 9m^2) r_O^2 + 8a^6} = \frac{27m^2}{r_O^2} \left(1 + O\Big(\frac{m}{r_O}\Big)\right)$$

A. Grenzebach, VP, C. Lämmerzahl:
Int. J. Mod. Phys. D 24, 1542024 (2015)

Up to terms of order $O\Big(\dfrac{m}{r_O}\Big)$, Synge's formula is still correct for the vertical diameter of the shadow

Shadow of black hole with $a = m$ for observer at $r_O = 5m$

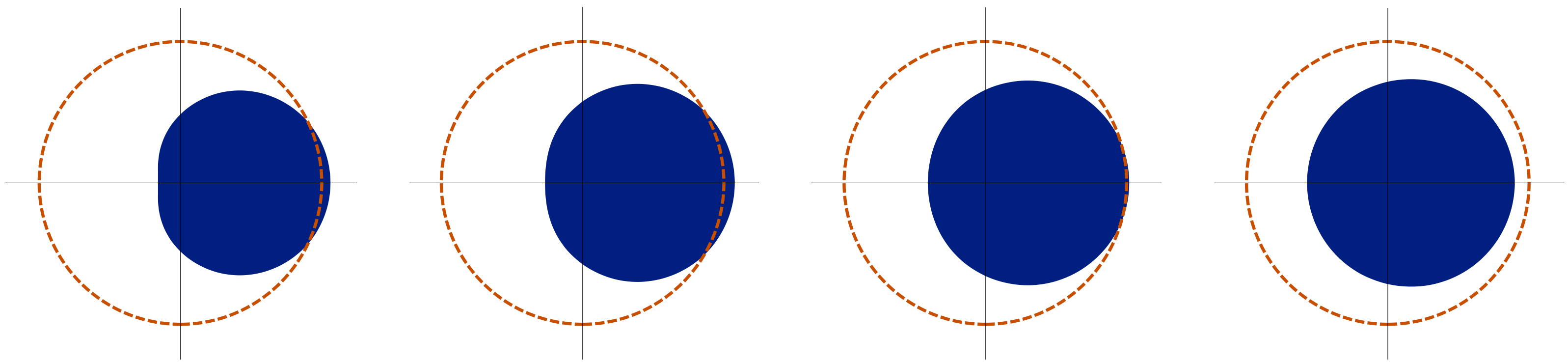

$\vartheta_O = \frac{\pi}{2}$ $\vartheta_O = \frac{3\pi}{8}$ $\vartheta_O = \frac{\pi}{4}$ $\vartheta_O = \frac{\pi}{8}$

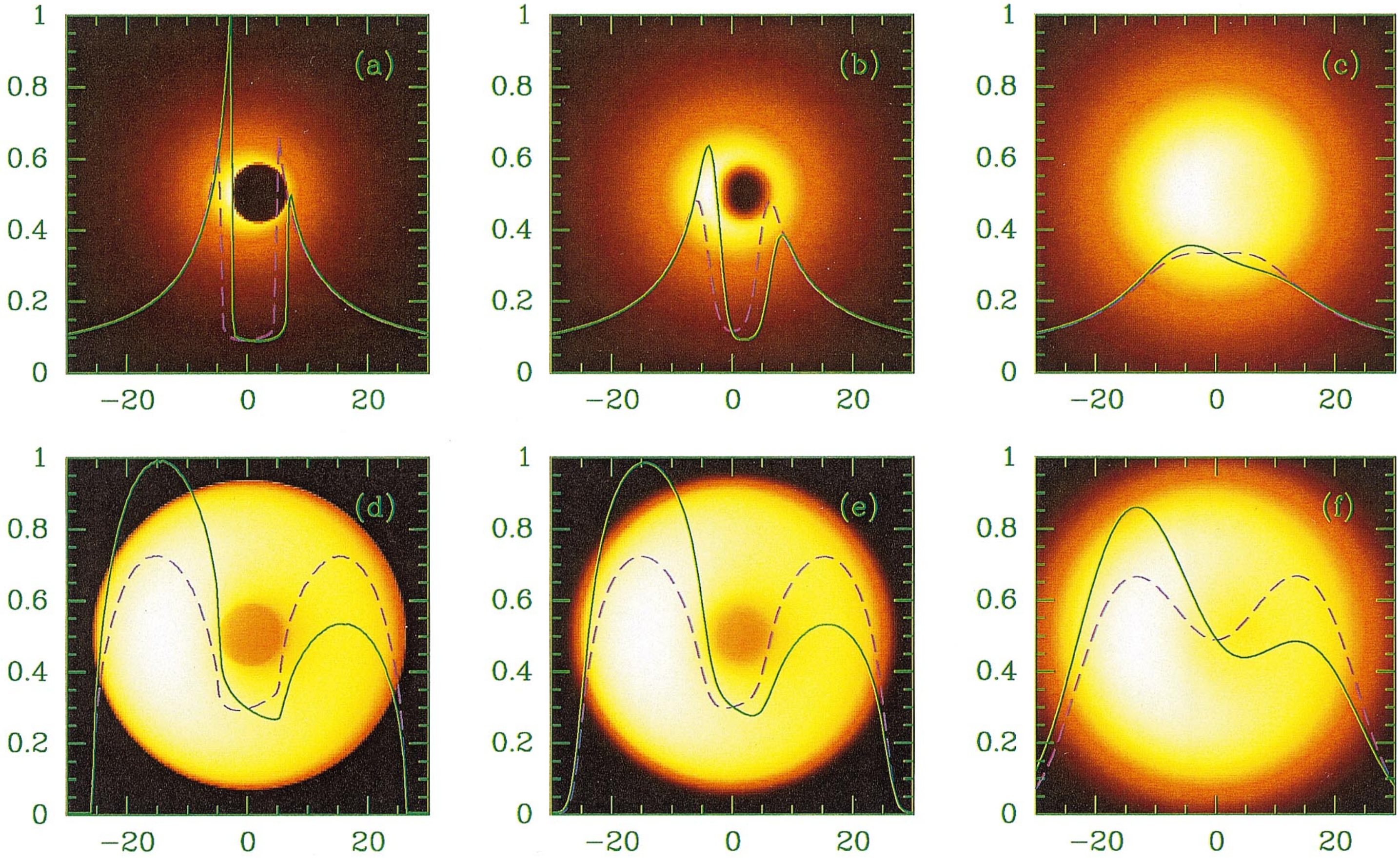

From H. Falcke, F. Melia and E. Agol: Astrophys. J. 528, L13 (2000)

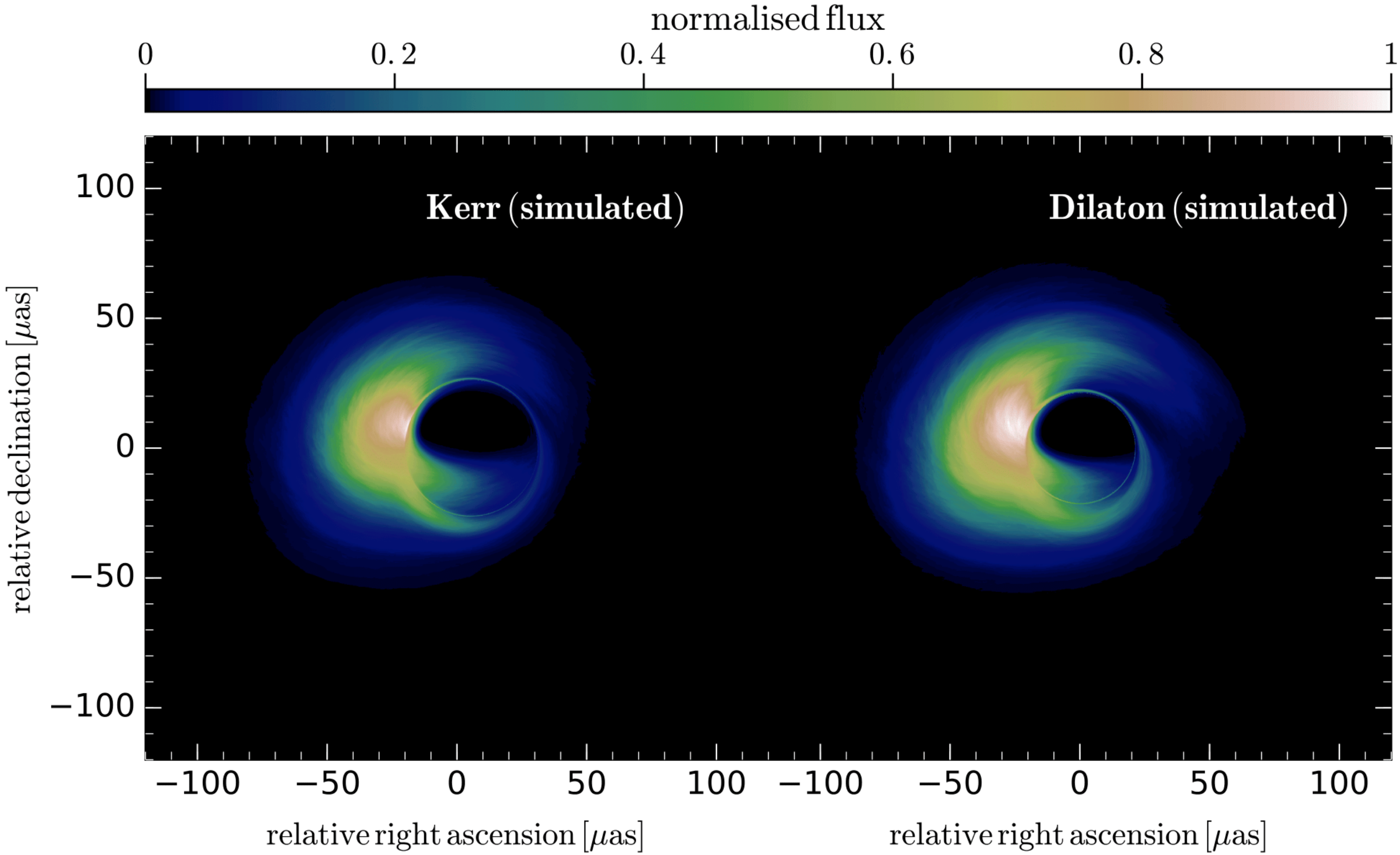

From Y. Mizuno, Z. Younsi et al.:
Nature Astronomy 2, 585 (2018)

Analytic formula for the shadow in a plasma on Kerr

VP, O. Yu. Tsupko: Phys. Rev. D 95, 104003 (2017)

Example: $\omega_p(r,\vartheta)^2 = \dfrac{\omega_c^2\sqrt{m^3 r}}{r^2 + a^2\cos^2\vartheta}\,, \qquad \omega_c = \text{constant}$

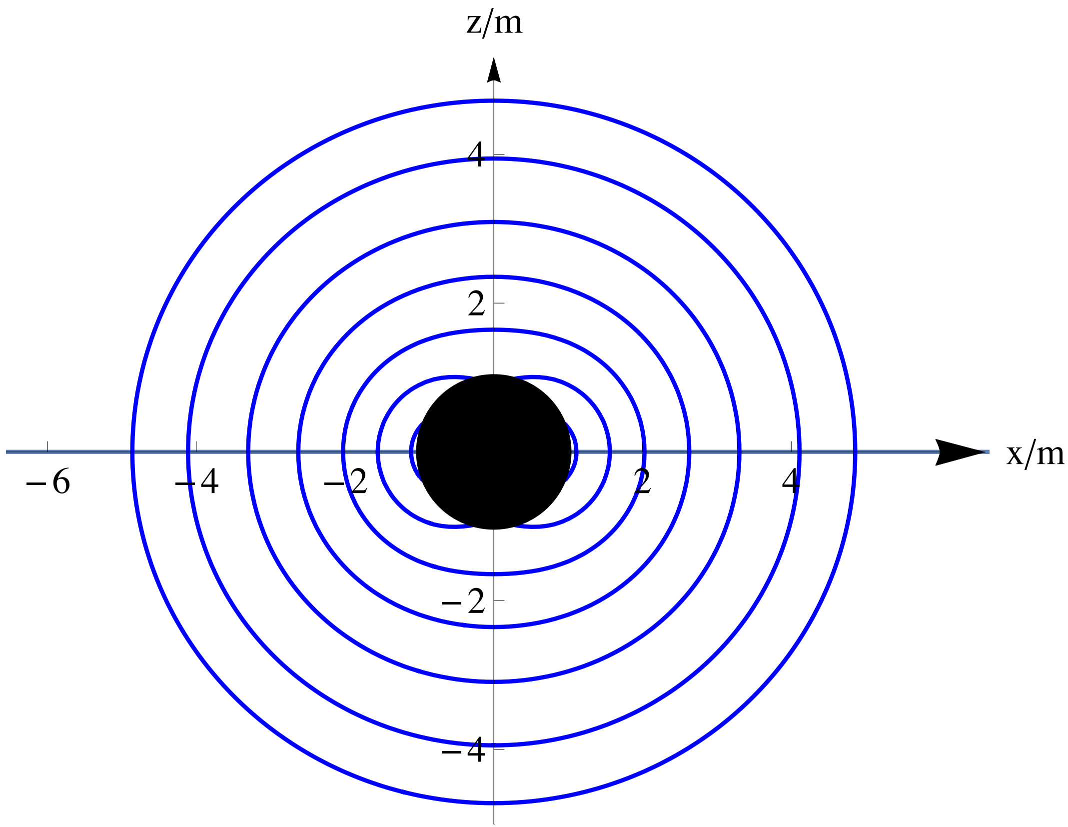

Photon region, $a = 0.999\,m$, $\omega_c^2/\omega_0^2 = 14.5$

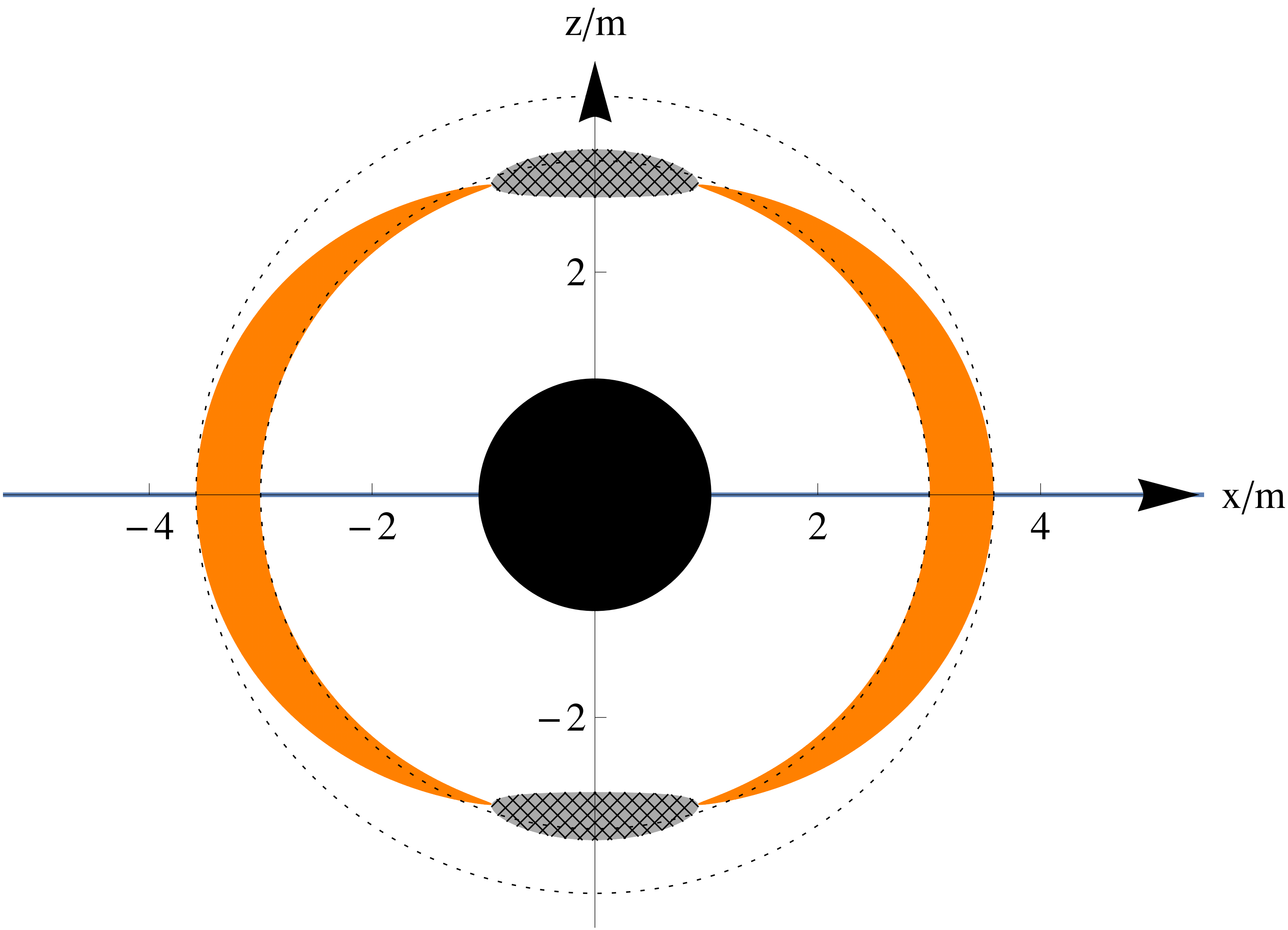

Shadow, $a = 0.999\, m, r_O = 5\, m\,,\ \vartheta_O = \pi/2$

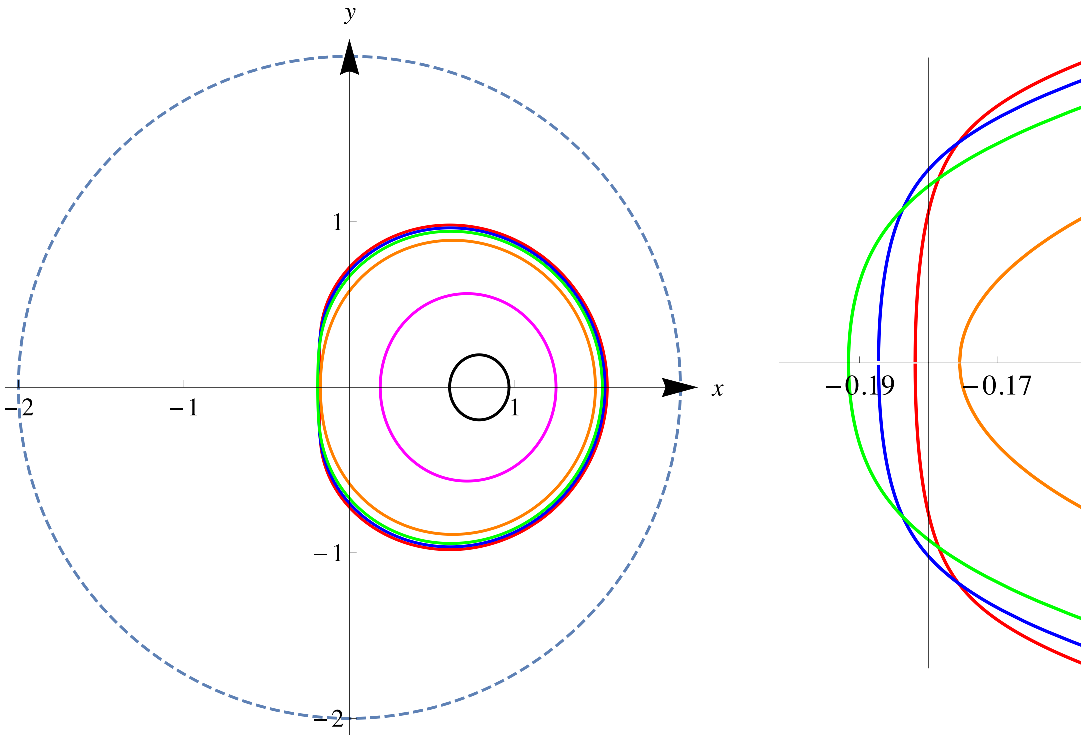

Shadow shrinks with increasing ω_c^2/ω_0^2